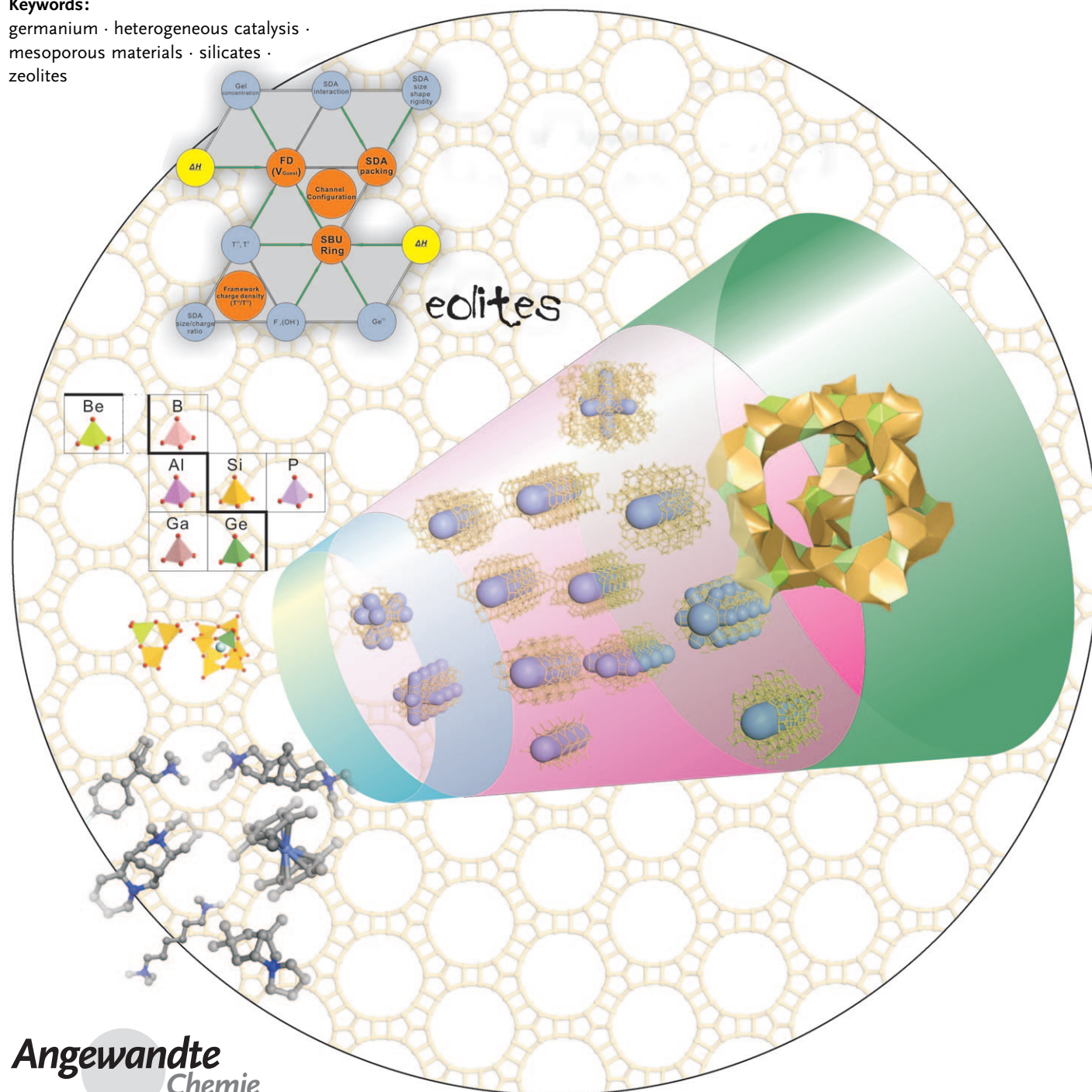


Extra-Large-Pore Zeolites: Bridging the Gap between Micro and Mesoporous Structures

Jiuxing Jiang, Jihong Yu, and Avelino Corma*

Keywords:

germanium · heterogeneous catalysis · mesoporous materials · silicates · zeolites



The conditions required to produce zeolites with low framework density and extra-large pores are discussed. Correlations between framework stability and geometrical and topological descriptors are presented. An attempt has been made to rationalize the synthesis of extra-large-pore zeolites in terms of the synthesis mechanism, the directing effect of the organic structure directing agent (OSDA), the framework atoms, and the gel concentration. Extra-large-pore zeolites, including the recently discovered chiral mesoporous ITQ-37, are described and their catalytic and adsorption properties discussed. Finally, strategies are presented for the preparation of extra-large-pore zeolites with different pore topologies that can fulfill pre-established catalytic and adsorption targets.

1. Introduction

Zeolite materials are an important class of crystalline inorganic microporous solids formed by TO_4 tetrahedra (T = Si, P, Al, Ge, Ga, etc) with a well-defined regular pore system. The most interesting features of zeolites lie in the variable chemical compositions of their pore walls, as well as the tunable pore diameters and pore geometries. These excellent characteristics make zeolites suitable for a wide range of applications in the fields such as adsorption, separation, catalysis,^[1–3] microelectronics,^[4] metal diagnosis,^[4] and, generally speaking, in any field where the host–guest chemistry defines the final behavior of the system. Zeolites are classified as having small, medium, large, and extra-large pore structures for pore windows delimited by 8, 10, 12, and more than 12 T-atoms, respectively.^[5–8] In the field of zeolites, the synthesis of materials with extra-large pores is still an important driving force for the development of new structures.^[5] In this Review, we will focus on the synthesis and applications of extra-large pore zeolites.

2. Extra-Large-Pore Crystalline Microporous Molecular Sieves

2.1. Non-Zeolitic Crystalline Microporous Materials

2.1.1. Phosphates

The history of crystalline materials with extra-large pores can be traced back to the mineral cacoxenite,^[9] a hydrated basic iron(III) oxyphosphate with a pore diameter of 1.5 nm. However, cacoxenite can not be considered as a real zeolite, or even a zeotype material, since it contains Fe^{III} ions octahedrally coordinated with oxygen atoms. Meanwhile the interest of this microporous crystalline material is limited because the structure collapses after removal of the guest water molecules by calcination. The first real zeotype material with more than 12 T atoms in the rings is the aluminophosphate molecular sieve (AlPO_4) VPI-5^[10] with 18-membered ring (18R) channels with a 1.2 nm pore diameter. This material, upon heating in the presence of moisture, was


From the Contents

1. Introduction	3121
2. Extra-Large-Pore Crystalline Microporous Molecular Sieves	3121
3. Attempts to Predict New Zeolite Structures	3123
4. Preparation of Low-Framework-Density, Large-Pore Zeolites	3124
5. Producing Extra-Large-Pore Zeolites	3127
6. Synthesis of Extra-Large-Pore Zeolites	3132
7. Synthesis of a Mesoporous Chiral Zeolite	3133
8. Germanium-Containing Zeolites: Limitations and Potential Solutions	3134
9. Adsorption and Catalysis	3134
10. Summary and Outlook	3141

transformed into $\text{AlPO}_4\text{-}8$ ^[11] with one-dimensional (1D) 14R channel system. The work on VPI-5 encouraged researchers to search for other phosphate-based molecular sieves with extra-large pores. Along this line, researchers at Jilin University and the Davy Faraday Research Laboratory reported the synthesis of a 20R channel aluminophosphate JDF-20.^[12] Since then a number of extra-large-pore crystalline microporous metal phosphates have been prepared. Estermann and co-workers^[13] reported the synthesis of a 3D 20R channel gallophosphate molecular sieve named Cloverite. This material has a framework density of 11.1 T atoms per 1000 Å³, and could be calcined up to 700 °C while preserving the structural integrity. A series of gallophosphates and fluorinated gallophosphates with 14R to 24R channels has also been synthesized.^[14–22] Other crystalline metal phosphates (ZnPO , InPO , VPO , FePO , CoPO , and NiPO) with up to 24R channels have been reported in the last two decades, and a summary of their

[*] J. Jiang, Prof. A. Corma
 Instituto de Tecnología Química (UPV-CSIC)
 Universidad Politécnica de Valencia
 Avenida Los Naranjos s/n, 46022 Valencia (Spain)
 Fax: (+34) 96-3877809
 E-mail: acorma@itq.upv.es

J. Jiang, Prof. J. Yu
 State Key Laboratory of Inorganic Synthesis and Preparative Chemistry, College of Chemistry, Jilin University
 Changchun 130012 (China)

 Supporting information for this article is available on the WWW under <http://dx.doi.org/10.1002/anie.200904016>.

structures together with chemical compositions, pore diameters, and the structure-directing agents (SDAs) used for the synthesis is given in Table 1. Notice that many of the materials reported in Table 1 have very limited thermal stability. Nevertheless some of them are stable upon calcination and show adsorption and even catalytic properties. For instance, two vanadium phosphates^[23] with pores formed by 16R and 8R windows can adsorb water. Nickel phosphates VSB-1^[24] and VSB-5^[25] with 24R channels remain stable upon removal of the SDAs and show some catalytic properties.

However, in most of these materials, and certainly in those with 18R, 20R, or 24R pores, the frameworks contain penta- and/or hexa-coordinate atoms and can not be considered as zeotype structures. The higher coordination number of a framework atom can reduce the geometric stress generated by four-coordinate atoms in a traditional zeolite. As a result, the formation of these extra-large pore materials is facilitated by increasing the coordination number of some framework cations.

2.1.2. Phosphites and Organic Phosphates

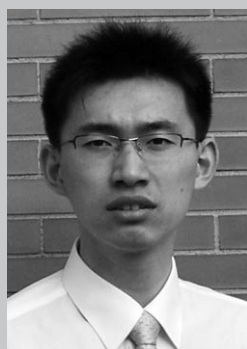
The phosphate tetrahedra in metal phosphates can be replaced by pseudo-pyramidal phosphite units, HPO_3^{2-} , or organic phosphate groups, $-\text{CPO}_3$, forming microporous phosphites and organophosphates (see Table 2). A series of microporous zinc phosphites with 16R pores has been synthesized,^[26–29] including FJ-14^[28] which has interesting magnetic properties. Vanadium, cobalt, and zinc phosphites with channels made of 14R, 16R, 18R,

Table 1: Microporous phosphates with extra-large pores.^[a]

Material	Formula	Max. Pore Dimension	SDA	Ref.
VBPO-CJ27	$[\text{DIPYR}]_{0.87}[\text{PYR}]_{0.28}[\text{Ga}_7(\text{PO}_4)_6\text{F}_3(\text{OH})_2] \cdot 2 \text{H}_2\text{O}$	14	1	[19]
	$[\text{NH}_3(\text{CH}_2)_3\text{NH}_3]_4[\text{H}_3\text{O}]_3[\text{In}_9(\text{PO}_4)_6(\text{HPO}_4)_2\text{F}_{16}] \cdot 3 \text{H}_2\text{O}$	14	5	[190]
	$\text{Na}_2[\text{VB}_3\text{P}_2\text{O}_{12}(\text{OH})] \cdot 2.92 \text{H}_2\text{O}$	16	Na^+ ion	[191]
ULM-5	$[\text{HN}(\text{CH}_2\text{CH}_2)_3\text{NH}]_{\text{K}1.35}[\text{V}_5\text{O}_9(\text{PO}_4)_2] \cdot x \text{H}_2\text{O}$	16	2	[23]
	$\text{Cs}_3[\text{V}_5\text{O}_9(\text{PO}_4)_2] \cdot x \text{H}_2\text{O}$	16	Cs^+ ion	[23]
ULM-15	$[\text{C}_4\text{N}_3\text{H}_{16}]_3[\text{Co}_6(\text{PO}_4)_5(\text{HPO}_4)_3] \cdot \text{H}_2\text{O}$	16	3	[192]
ULM-16	$[\text{H}_3\text{N}(\text{CH}_2)_6\text{NH}_3]_4[\text{Ga}_{16}(\text{PO}_4)_{14}(\text{HPO}_4)_2(\text{OH})_2\text{F}_7] \cdot 6 \text{H}_2\text{O}$	16	4	[14]
MIL-31	$[\text{H}_3\text{N}(\text{CH}_2)_3\text{NH}_3][\text{Fe}_4\text{F}_3(\text{PO}_4)_4(\text{H}_2\text{O})_4]$	16	5	[193]
	$[\text{NC}_5\text{H}_{12}]_{1.5}[\text{H}_3\text{O}]_{0.5}[\text{Ga}_4(\text{PO}_4)_4\text{F}_{1.33}(\text{OH})_{0.67}] \cdot 0.5 \text{H}_2\text{O}$	16	6	[15, 16]
MIL-46	$[\text{NH}_3(\text{CH}_2)_2\text{NH}_2(\text{CH}_2)_2\text{NH}_3]_2[\text{NH}_2(\text{CH}_2)_2\text{NH}_2(\text{CH}_2)_2\text{NH}_2]$	16	3	[194]
MIL-50	$[\text{In}_{6.8}\text{F}_8(\text{H}_2\text{O})_2(\text{PO}_4)_4(\text{HPO}_4)_4] \cdot 2 \text{H}_2\text{O}$	18	7 ^[b]	[17]
Cloverite	$[\text{N}_2\text{C}_{10}\text{H}_{26}]_2[\text{Ga}_9(\text{PO}_4)_9\text{F}_3(\text{OH})_2(\text{H}_2\text{O})] \cdot 2 \text{H}_2\text{O}$	18	6	[16]
JDF-20	$[\text{N}_2\text{C}_6\text{H}_{18}]_2[\text{Rb}]_2[\text{Ga}_9(\text{PO}_4)_8(\text{HPO}_4)(\text{OH})\text{F}_6] \cdot 7 \text{H}_2\text{O}$	18	4	[18]
ICL-1	$[\text{RF}]_{192}[\text{Ga}_{768}\text{P}_{768}\text{O}_{2976}(\text{OH})_{192}]$	20	8	[13]
	$[\text{N}_2\text{Et}_3\text{NH}][\text{Al}_5\text{P}_6\text{O}_{24}\text{H}] \cdot 2 \text{H}_2\text{O}$	20	9	[12]
ND-1	$[\text{NH}_3(\text{CH}_2)_6\text{NH}_3][\text{Zn}_4(\text{PO}_4)_2(\text{HPO}_4)_2] \cdot 3 \text{H}_2\text{O}$	20	4	[195]
	$[\text{NH}_3(\text{CH}_2)_4\text{NH}_3]_2[\text{Ga}_4(\text{HPO}_4)_2(\text{PO}_4)_3(\text{OH})_2\text{F}] \cdot 6 \text{H}_2\text{O}$	20	10	[20]
NTHU-1	$[\text{NH}_3(\text{CH}_2)_3\text{NH}_3]_2[\text{Fe}_4(\text{OH})_3(\text{HPO}_4)_2(\text{PO}_4)_3] \cdot x \text{H}_2\text{O}$	20	5	[196]
	$[\text{NH}_3(\text{CH}_2)_4\text{NH}_3]_2[\text{Ga}_4(\text{HPO}_4)_2(\text{PO}_4)_3(\text{OH})_3] \cdot \gamma \text{H}_2\text{O}$	20	10	[21]
VSB-1	$[\text{H}_2\text{DACH}][\text{Zn}_3(\text{PO}_4)_2(\text{PO}_3\text{OH})] \cdot 2 \text{H}_2\text{O}$	24	11	[197]
	$[(\text{C}_4\text{N}_3\text{H}_{16})(\text{C}_4\text{N}_3\text{H}_{15})][\text{Fe}_5\text{F}_4(\text{H}_2\text{PO}_4)(\text{HPO}_4)_3(\text{PO}_4)_3] \cdot \text{H}_2\text{O}$	24	3	[198]
VSB-5	$[\text{Ga}_2(\text{DETA})(\text{PO}_4)_2] \cdot 2 \text{H}_2\text{O}$	24	3	[22]
	$[(\text{H}_3\text{O}, \text{NH}_4)]_4[\text{Ni}_{18}(\text{HPO}_4)_4(\text{OH})_3\text{F}_9] \cdot 12 \text{H}_2\text{O}$	24	No template	[24]
	$[(\text{OH})_{12}(\text{H}_2\text{O})_6][\text{Ni}_{20}(\text{HPO}_4)_8(\text{PO}_4)_4] \cdot 12 \text{H}_2\text{O}$	24	5 ^[b]	[25]

[a] DIPYR = 4,4'-dipyridine, PYR = dipyridine, Rb = rubidium ion, RF = quinuclidinium fluoride, DACH = 1,2-Diaminocyclohexane, DETA = Diethylenetriamine. [b] Only one example.

and 26R have recently been reported.^[30–33] For example, the open framework of ZnHPO-CJ1 is made up of strictly alternating ZnO_4 tetrahedra and HPO_3 pseudo-pyramids forming parallel 24R and 8R channels extending along the crystallographic *c* axis. The approximate size of the 24R window is $11.0 \times 11.0 \text{ \AA}$.^[32] Of the organic phosphates, a 24R organic phosphate is worth mentioning as the only example of



Jiuxing Jiang, received BS from Jilin University, and then joined Prof. Ruren Xu and Prof. Jihong Yu as a Ph.D. student. In 2007 he won a grant of China Scholarship Council to go to the Instituto de Tecnología Química (UPV-CSIC) to continue Ph.D. work with Prof. Corma. His research interests focus on the synthesis and applications of novel zeolites using high throughput techniques.



Jihong Yu obtained his Ph.D. (1995) from Jilin University, and worked as a postdoctoral fellow first at the Hong Kong University of Science and Technology and then at Tohoku University, Japan (1996–1998). Since 1999 she has been a full Professor in the Chemistry Department, Jilin University, and holds the Cheung Kong Professorship. Her research is on the design and synthesis of zeolites and related inorganic open-framework materials. She has been the Editor of the journal of Microporous and Mesoporous Materials since 2008.

Table 2: Microporous phosphites and organic phosphates with extra-large pores.^[a]

Material	Formula	Max. Pore Dimension	SDA	Ref.
FJ-14	$(C_5N_2H_{14})[(VO \cdot H_2O)_3(HPO_3)_4] \cdot H_2O$	14	12	[30]
	$(NC_5H_{12})_2[Zn_3(HPO_3)_4]$	16	13	[26]
	$[CN_4H_7]_2[Zn_3(HPO_3)_4]$	16	14	[27]
	$Ni(DETA)Zn_2(HPO_3)_3(H_2O)$	16	3	[28]
CoHPO-CJ2	$[Zn(H_2O)_6][Zn_3(HPO_3)_4]$	16	15	[29]
	$(H_3O)_2[Co_8(HPO_3)_9(CH_3OH)_3] \cdot 2H_2O$	18	3	[31]
ZnHPO-CJ1	$(C_4H_{12}N)_2[Zn_3(HPO_3)_4]$	24	16	[32]
NTHU-5	$[(NH_3CH_2CH_2NH_3)(btc)][Zn_3(O_3PCH_2COO)_2(O_3PCH_2COOH)]$	24	17	[34]
	$(C_4H_9NH_3)_2[AlFZn_2(HPO_3)_4]$	26	16	[33]

[a] btc = 1,3,5-benzenetricarboxylic acid.

an extra-large-pore species in the family.^[34] Unfortunately, because of their poor stability, none of these materials retains its pore structure when the guest is removed by calcination and consequently their application is limited.

2.1.3. Germanates

Extra-large-pore structures have been found in many germanates. The germanium atom can be bound to four, five, or six oxygen atoms forming various cluster building units. In 2001, Plevert et al.^[35] and Zhao et al.^[36] reported two 24R channel germanates, ASU-16 and FDU-4, respectively. ASU-16 has a very low framework density (8.6 Ge atoms per 1000 Å³) and FDU-4 has an interesting 3D channel system, in which each 24R channel is surrounded by six 12R channels, and both are connected by alternating 8R pore windows. Other germanates and nickel germanates with 14 × 12 × 12R^[37] and 24R^[38] pores have been reported. Deserving special mention is a series of germanates of the SU family. Among them, SU-M and its chiral derivative SU-MB,^[39] both have 30R pores and a maximum pore opening of 2.5 nm. However, owing to the presence of cations in the pores, the pore volume is low and the Brunauer–Emmett–Teller (BET) surface area is approximately 300 m² g⁻¹. The thermostability of these materials is also very limited, and the structures are only maintained up to 320 °C.



Avelino Corma studied chemistry at the Universidad de Valencia and received his Ph.D. at the Universidad Complutense de Madrid in 1976. He was a Postdoc in the Department of chemical engineering at the Queen's University (Canada, 1977–1979) and has been the director of the Instituto de Tecnología Química (UPV-CSIC) at the Universidad Politécnica de Valencia since 1990. His current research field is catalysis, covering aspects of synthesis, characterization, and reactivity in acid–base and redox catalysis. He is co-author of more than 700 articles and 100 patents on these subjects.

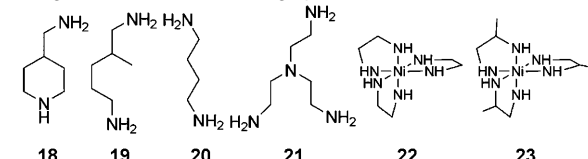
SU-61^[40] has a 1D 26R channel system. Interestingly, if SU-M is considered to be the counterpart of MCM-48, then SU-61 would be the counterpart of MCM-41. SU-8 and SU-44^[41] have 16R and 18R channels, respectively. More recently, Yu et al.^[42] reported a mesoporous crystalline germanate JLG-12 with 30R channels. It has a mesopore of 1.3 × 2.2 nm in diameter, which is comparable to those of the 30R pores (1.0 × 2.2 nm) in SU-M. All these germanates with extra-large pores (see Table 3) contain germanium atoms in mix coordination environments. None of the frameworks is stable, they collapse when the guests are removed by calcination.^[35,36,39,43]

2.2. Extra-Large-Pore Zeolites

UTD-1^[44] was the first high-silica zeolite to have 1D 14R channels. Its discovery was followed by another 1D 14R pure silica zeolite named CIT-5.^[45] Later, Cheetham et al. reported the synthesis of beryllsilicates OSB-1^[46] that has a system of 14R parallel pores that are chiral and formed by a double-helix 3R chain. 14R extra-large-pore borosilicate zeolites (SSZ-53 and SSZ-59) were reported by researchers at Chevron^[47] and an 18 × 8 × 8R gallosilicate zeolite (ECR-34) with a pore diameter of 1.08 nm for the 18R was reported by Strohmaier and Vaughan.^[48] A germanosilicate zeolite with very large pore volume was first reported in the patent literature as ITQ-15,^[49] which has a channel system formed by 14 × 12R pores^[50,51] and has been assigned as zeotype UTL. Recently, Corma et al. reported a silicogermanate zeolite (ITQ-33)^[52] with an 18 × 10 × 10R pore system that will be discussed in Section 6. To date, the number of extra-large-pore zeolites synthesized is rather limited and it would be of interest to predict potential new structures, to study their stability, and then to design organic structure-directing agents (OSDAs) that can lead to the formation of such structures.

3. Attempts to Predict New Zeolite Structures

Early work directed to the prediction of potential extra-large-pore zeolite structures was mainly based on intuitive model building. Noticeable work was done by Breck^[53] who predict the existence of the enigmatic “Breck structure 6”, the twinned polytype of the FAU framework. This structure was later synthesized and is now known as EMT. Barrer and Villiger^[54] presented a series of hypothetical structures related to zeolite L (LTL), with 24R pores and a diameter of approximately 1.5 nm. Some of these structures consist of known building units that do not violate crystal chemistry constraints. Smith and Dytrych^[55] illustrated several nets constructed by 4R and larger rings with channels of unlimited

Table 3: Microporous germanates with extra-large pores.^[a]


Material	Formula	Max. Pore Dimension	SDA	Ref.
ICMM7	$(C_6N_2H_{16})_2[Ge_{13}O_{26}(OH)_4](H_2O)_{1.5}$	14	18	[37]
SU-8	$(C_6H_{16}N_2H_2)_5[Ge_9O_{18}(OH)_4][Ge_7O_{15}(OH)]_2[GeO(OH)_2]_2$	16	19	[41]
SU-44	$(C_6H_{16}N_2H_2)_{10}[Ge_9O_{18}X_4][Ge_7O_{15}X_2][GeOX_2]_{2.85}$	18	19	[41]
ASU-16	$(H_2dab)_3(dab)_{0.5}[Ge_{14}O_{29}F_4] \cdot 16 H_2O$	24	20	[35]
FDU-4	$[N(CH_2CH_2NH_2)_3]_{2/3}[HCON(CH_3)_2]_{1/6} \cdot [Ge_9O_{17}(OH)_4](H_2O)_{11/3}$	24	21	[36]
FJ-1a	$[2Ni(en)_3][Ni@Ge_{14}O_{24}(OH)_3]$	24	22	[38]
FJ-1b	$[Ni(enMe)_3]_2[Ni@Ge_{14}O_{24}(OH)_3]$	24	23	[38]
SU-61	$[C_6H_{16}N_2H_2]_2[Ge_{8.7}Si_{1.3}O_{16}O_{11/2}OH][Ge_{0.71}Si_{0.29}O_{4/2}] \cdot [Ge_{0.22}Si_{0.78}O_{3/2}OH]_2$	26	19	[40]
SU-M	$[(H_2MPMD)_2(H_2O)_4][Ge_{10}O_{20.5}(OH)_3]$	30	19	[39]
SU-MB	$[(H_2MPMD)_{5.5}(H_2O)_4][Ge_{10}O_{21}(OH)_2][Ge_7O_{14}F_3]$	30	19	[39]
JLG-12	$[C_6N_2H_{18}]_{30}[Ge_9O_{18}X_4]_6[Ge_7O_{14}X_3]_4[Ge_7O_{14.42}X_{2.58}]_8[GeX_2]_{1.73} \cdot (X = OH, F)$	30	19	[42]

[a] dab = diaminobutane, en = ethylenediamine, enMe = 1,2-diaminopropane, MPMD = 2-methylpentamethylenediamine.

diameter. Furthermore, Smith^[56] described a great number of frameworks that were constructed using systematic methods.

In the last decade there has been significant progress in the development of efficient computer methods for predicting new hypothetical zeolite frameworks.^[57–62] Recently, Treacy and co-workers^[63] used a symmetry constrained bond-searching method and were able to generate over two-million structures with $n_T < 4$ (n_T : number of topologically independent vertices) for all the space groups, and $4 \leq n_T \leq 7$ for some high-symmetry space groups. Earl and Deem^[57d] used simulated annealing to generate several-million hypothetical structures, of which 450 000 are potentially stable when their calculated lattice energies are compared with those of known zeolite structures. Based on recent advances on mathematical tiling theory, Klinowski and co-workers^[59a] established a way to generate four-connected unimodal, bimodal, and trinodal networks. Férey and co-workers predicted a series of not-yet synthesized framework topologies with the AASBU (automated assembly of secondary building unit) method.^[60] Another approach to the prediction of hypothetical zeolite frameworks has been proposed by Yu and co-workers^[61] who were able to generate a series of new zeolite frameworks with specified pore geometries, by defining a forbidden zone where the framework atoms cannot reside.

Though extensive work has been carried out to predict new hypothetical structures, there are still many unsolved problems in this area. Particularly, the generation of hypothetical frameworks with multiple nodes as found in complex zeolite structures, such as IM-5(IMF) and TNU-9(TUN) with 24 distinct T-atoms,^[64–66] is a big challenge for current computation facilities. However, the method of framework generation in density maps (FGDM) developed recently by researchers in Jilin University and ETH Zurich has recently

facilitated the process of the complex zeolite framework generation.^[66] On the other hand, many hypothetical zeolites have high lattice energies that are not chemically feasible. To date, there are two main databases of hypothetical zeolite structures available online.^[63,67] The database developed by Treacy^[63] gives a huge number of hypothetical structures and has been successful in predicting the existence of ITQ-33. However, the size of the channel cannot be queried in this database. The other database was built up by Li and Yu et al. in Jilin University with the aim of collecting hypothetical zeolite frameworks with specified pores.^[67] This database allows pore information, such as accessible volume, cavity type, channel dimension, and channel orientation, to be queried. Currently 52 hypothetical zeolite frameworks with extra-large pores can be found in this database

(see Supporting Information) and one of them contains 42R channels.

In summary, there are still many hypothetical extra-large-pore zeolites with the potential to be synthesized. The question is why only a small portion of theoretically feasible structures can be synthesized? Is this due to the unavoidable decrease in the stability when the pore volume of the zeolite is increased? Maybe more sophisticated synthesis methods and novel SDAs are needed for experimental synthesis to catch up with the theoretical prediction.

4. Preparation of Low-Framework-Density, Large-Pore Zeolites

The framework density (FD), that is, the number of T-atoms per 1000 Å³ of the material, can be used as a descriptor to distinguish zeolites from denser tectosilicates. While there is a relationship between FD and zeolite pore volume in that lower FD corresponds to a higher micropore volume, it does not follow that a large micropore volume in a zeolite indicates large pores. However, there is no doubt that zeolites with extra-large pores and three-dimensional pore topologies will certainly have large pore volumes. To date, FD values lower than 12 have only been found for two frameworks in the IZA structure database,^[69] these are the interrupted framework (CLO) and the chalcogenide UCR-20^[68] (RWY); such values have also been found for some hypothetical frameworks. This situation is remarkable taking into account that 191 frameworks have been synthesized to date. The question then is, why zeolites with low FD and, moreover, zeolites with multidimensional extra-large pores have been so elusive?

In 1989, Brunner and Meier^[70] carried out a topological analysis on over 70 natural or synthetic silicate and aluminophosphate materials with four-connected frameworks. They found that when the frameworks are grouped together as a function of the smallest ring contained (Figure 1 a), the minimum FD_{Si} (the framework density calculated for an idealized SiO_2 composition) for each of the groups decreases with the smallest ring size. This statistical work inspired the researchers to switch the synthesis target from low-framework-density zeolites towards structures with 3R or 4Rs. In their work, Brunner and Meier considered only around 70 zeolite frameworks. The number of structures has increased since then, and 191 structures (data taken from IZA website)^[69c] are plotted in Figure 1 b. It can be seen that the same type of correlation still applies. Though the minimum FD achieved is now from Tschörtnerite (TSC) rather than Faujasite (FAU), ITQ-26(IWS) rather than Beta, and ZSM-

39(MTN) rather than ferrierite (FER) structures. Nevertheless the linearity is still maintained. The Nitridophosphate-1(NPO) and OSB-1(OSO) fill the earlier blank for the 3R group, and the 3R-and-larger ring group has also been enriched. Notably, ITQ-33 gives, for now, the lowest FD. Furthermore, the linear extrapolation implies that ITQ-33 and OSB-1 are not the lowest FD zeolites that can be obtained.

Data have also been plotted in Figure 1 b for hypothetical extra-large-pore structures taken from the database of Jilin University (For more details see the Supporting information and Ref. [67]) In Figure 1 b it can be seen that some extra-large-pore zeolite structures can be very dense. For instance, the FD value of H184-3 is 23.77 T atoms per 1000 \AA^3 . However, this feature does not prevent the structure from having an extra-large-pore system (see Supporting information). For every group the plot shows a random distribution,

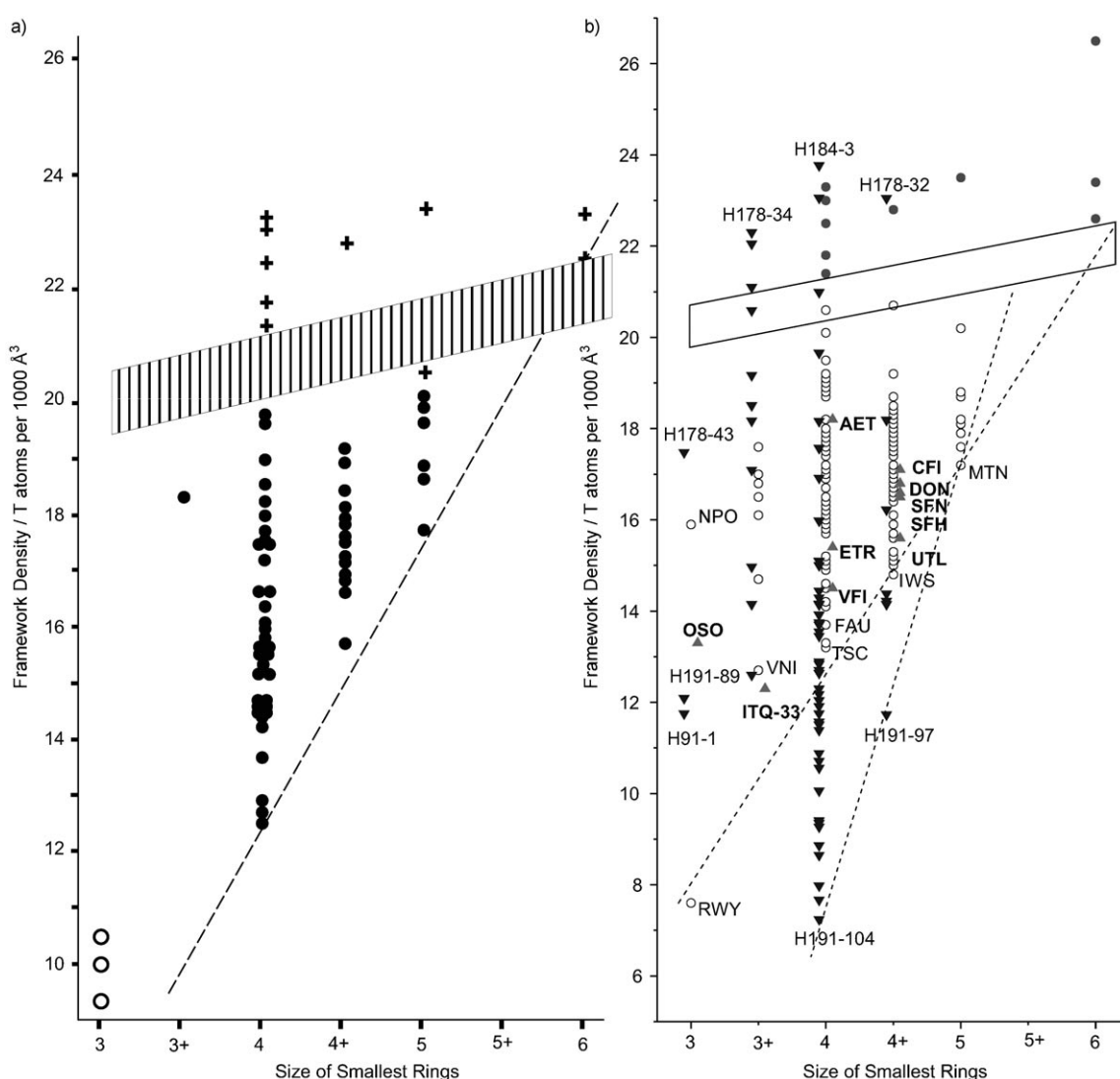


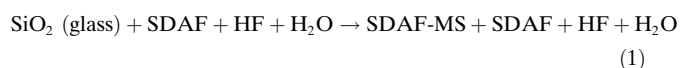
Figure 1. Distribution of framework density (FD) versus size of smallest ring in the framework. The FD values are taken from the *Atlas of Zeolite Framework Types*.^[69] CLO, RON, WEN, LIT, PAR, and CHI are excluded due to their interrupted structure. Framework types: a) + dense framework; ● zeolite; ○ hypothetical. b) ○ normal zeolite; ● mineral; ▲ real ELP structure; ▼ hypothetical ELP structure. ELP = extra-large pore. Dotted lines indicate the linearity for real ELP zeolites and hypothetical ELP zeolites. Parallelogram indicates the gap between zeolite and dense framework. Figure 1 a taken from Ref: [70].

indicating that there is not a correlation between FD and the presence or not of extra-large pores in the structure. Therefore, it can be concluded that a linear correlation between FD and the size of smallest ring is not mandatory, and such a correlation may change with the discovery of new structures. Nevertheless, it appears, to date, that both synthesized and simulated zeolite structures with lower FD have a large number of 3- and 4-membered rings. Furthermore, Figure 1 clearly shows that a lower FD zeolite may contain multidimensional channels (FAU (Faujasite) 3D 12R, IWS (ITQ-26) 3D 12R) and/or cages (TSC (Tschörtnerite) and (ZSM-39(MTN)) but not necessarily extra-large pores. Therefore, a low FD is not a necessary condition for making an extra-large-pore zeolite, but three-dimensional extra-large-pore zeolites, such as ITQ-33, will have a low FD. Consequently, one feasible way to obtain extra-large-pore zeolites is to synthesize zeolite structures with a large number of 3- and 4-membered rings giving rise to very low FD (Figure 2, arrow 6). It is noted that the number of multidimensional extra-large-pore zeolites synthesized to date is small, and the number of zeolites synthesized with a large number of 4- and, especially, 3-membered rings in the framework is very low. This situation could be explained by the relative energy of the structures with or without many 3 and/or 4-membered rings, so that it has been possible to make extra-large-pore zeolites with low FD without including the smallest rings in the structure. Zwijnenburg and Bell^[71] recently carried out theoretical work based on the hypothetical structures in the databases. They have calculated the enthalpy of some extra-large-pore frameworks with extra-low FD containing only 4R and larger rings. The results show that there are no limits either from topological or from geometric and framework

energy aspects for preparing zeolite frameworks without 3 rings and giving extra-large-pore structures with extra-low framework density. According to their hypothesis, the lower limit of framework density given in Figure 1 is not an absolute value but a consequence of the limiting factors in synthesizing new materials. Nevertheless, their work mainly focused on the presence of 4-membered rings in the structure. It is not clear whether or not the density restriction exists for frameworks that contain neither 3- nor 4-membered rings.

4.1. The Intrinsic Stability of the Zeolite–Template System

Generally speaking, the interaction between the framework and the SDA template will stabilize the organic–inorganic composite of zeolitic material and, consequently, the stability of the whole system has to be considered first. Helmkamp and Davis^[72] and Piccione et al.^[73] measured the interaction energies of SDAs and several zeolites which were synthesized in fluoride media. To do this Equation (1) was considered where SDAF-MS represents the crystalline molecular sieve with enclathrated SDA⁺F⁻. No stoichiometric coefficients are given because they can be different for each synthesis, and the silica is assumed to be completely consumed.



An analysis of the thermodynamics shows that the process consist of three steps: 1) transformation of silica glass to a silica molecular sieve; 2) the partitioning of the SDA from the aqueous solution into the open framework; and 3) the dilution of the remaining SDAF and HF in solution during the synthesis. Piccione et al. showed that each of these steps contributed to the overall thermodynamics, and that no single factor dominated the overall Gibbs free energies.^[73] Additionally, the interaction energies have comparable contributions from enthalpy and entropy. For example, when tetrapropylammonium (TPA) and tetraethylammonium (TEA) were used to synthesize ZSM-5 (MFI) and Beta (*BEA), respectively, ΔH for TPA/MFI and TEA/*BEA were both $-3.2 \text{ kJ}(\text{mol SiO}_2)^{-1}$, whereas $T\Delta S$ for TPA/MFI and TEA/*BEA were 1.7 and 2.2 $\text{kJ}(\text{mol SiO}_2)^{-1}$, respectively. The small differences in the thermodynamic value for the different zeolites indicates that the self-assembly process depends upon the delicate interplay between a large number of weak interactions (as is often observed in biological systems), and this could be the driving force to the synthesis of a particular zeolite.^[72,73]

4.2. Stability of Template-Free Zeolite Structures

Since zeolites can only be used without the SDA guest, the stability of a structure after removal of the organic species is very important for its potential applications. Petrovic et al.^[74] first investigated the enthalpy of formation of various SiO_2

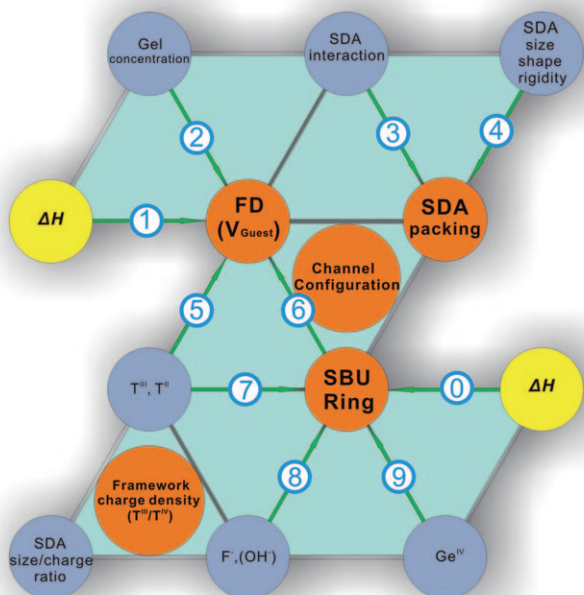


Figure 2. The relationships between the synthesis parameters (blue circle), structural parameters (orange circle), and thermodynamic factor (yellow circle). For ①–⑨ see text for details.

polymorphs (microporous zeolites and some dense phases) taking α -quartz as a reference, and Piccione et al.^[75] extended this work to include more zeolites. Their results show that when increasing the zeolite molar micropore volume (or when decreasing the framework density), the enthalpy of the zeolites increases (Figure 2, arrow 1). Relative to quartz the microporous silicas are metastable by 6.8–14.4 kJ mol⁻¹, and have similar stabilities to amorphous silicas and silica glasses.^[74,75] The energetic trends observed for pure-silica materials are also obtained for aluminophosphates. However, ordered mesoporous materials that are not crystalline show energy-independent behavior with increasing pore size (ca. 15 kJ (mol SiO₂)⁻¹ for pore sizes above 2 nm).^[76] Since the less-dense microporous crystalline materials give enthalpy values that are nearly the same as those of the ordered mesoporous materials, it would appear that thermodynamics do not necessarily limit the minimum FD that can be achieved with crystalline TO₄ frameworks.

4.3. Stability of Strained Structure Units: Correlation between Framework Stability and Geometrical and Topological Descriptors

Piccione et al.^[75] have correlated the effect of the presence of 3R and 4R in the structure on the enthalpy of the framework of pure-silica molecular sieves. According to calculations, 3R, 4R, and 5R are less stable than 6R by approximately 2.8, 1.1, and 0.08 kJ mol⁻¹, respectively^[75,77] (Figure 2, arrow 0). If this could be extrapolated to the zeolite structure, it would be expected that zeolites with 3R and 4R are less stable than zeolites with 5R and 6R. This situation would explain why a relatively small number of structures containing a large number of 3R and 4R have been synthesized. On the basis of these results a linear regression was established [$\Delta H_j = e_0 + \sum e_i f_{ij}$ ($i \neq 0$)] where f_{ij} is the fraction of ring type i present in structure j , and e_i is the energy contribution of ring type i (to be determined). As there were no pure silica materials with 3R prepared by direct synthesis available, only the effect of 4R was examined. The correlations found were no better than the energy correlations based on the framework density.

When the influence of a framework heteroatom (germanium) on the enthalpy of the of structures containing 4R was compared with those of the corresponding pure silica polymorphs,^[78] it was found that the germanosilicate zeolites were more metastable than the corresponding pure silica ones. All the zeolite frameworks examined became energetically less stable with increasing Ge content but the extent of the effect was different for each structure. This relationship can change completely when other structures compete as the synthesis product. In a further investigation^[79] of strained structure units, the zeolite framework was separated into face-sharing polyhedra, from which average face size and variance of the face-size distribution could be calculated. It was demonstrated that a correlation exists between viable zeolite structures and variance of the face-size distribution for a fixed average face size. This result represents a major advance that links the energy stability of framework structures to topo-

logical descriptors without an explicit consideration of geometric details. Nevertheless, the simple tiling prerequisite limits the possibilities and, furthermore, a considerable number of tile isomers (which correspond to non-viable structures) exist that do not follow the observed correlation. This situation indicates that it is necessary not only to consider strained structure units but also to consider the way they are connected to the framework. Sastre and Corma^[80] have investigated by means of theoretical calculations, what makes a structure stable or unstable and thus develop a more exact selection of variables. In their work, strained units (3R, cubic D4R) were inserted in real frameworks, and the results obtained were quite surprising. For instance, the Si sites corresponding to the 3R in ZSM-18^[81] are not the most strained, in fact the most unstable location in the framework for Si atoms corresponds to the positions in the 7R. The effect of strained D4R secondary building units was also evaluated. The results show that the energy contributions of D4R are different for different frameworks. For example, the energy contribution is high for BEC and LTA, and low for AST structures. Through the analysis of germanates with T₈O₂₀ units and the related silicates, O'Keeffe and Yaghi^[43] found that there are some topologies that are suitable for silicates but not for germanates, while others are suitable for germanates but not for silicates, and some are suitable for both types of materials. The results also explain why some zeolites with D4R units are easily prepared as a pure-silica form and others are not.

5. Producing Extra-Large-Pore Zeolites

When the field of zeolite synthesis started, the main objective was to find macroscopic correlations between the synthesis parameters and the formation of crystalline structures. Synthesis parameters mainly include crystallization time, temperature, and gel composition (T-atom source, SDA, mineralization agent, solvent, and concentration). When OSDAs were introduced to achieve zeolites with higher Si/Al ratio,^[82–84] it was found that the characteristics of the OSDA, which contributed to charge balance and pore filling, played a central role in determining the zeolite structure synthesized. These observations opened an intensive research in zeolite synthesis. The number of synthesis parameters increased and their influence on the structure established (see Figure 2).

5.1. The Role of OSDA in Zeolite Synthesis

It was soon intuitively predicted that the formation of a specific zeolite structure will be determined the self-assembly of the silica and the OSDA. Continuing in this direction, Gies et al.^[85,86] established a series of conditions that an organic molecule has to fulfill to be a successful OSDA to form clathrasil structures:

- 1) The molecule must be stable under the synthesis conditions.
- 2) The molecule should fit into the desired cage.

- 3) The molecule should form as many Van der Waals contacts as possible with the inner surface of the cage but with the least deformation.
- 4) The molecule should have only a weak tendency to form complexes with the solvent.
- 5) The molecule should be rigid because rigid molecules will tend to form clathrasils more easily than flexible molecules.
- 6) The tendency to form a clathrasil will increase with the increase in the basicity or polarizability of the guest molecule.

Clearly, most of these characteristics of OSDAs also apply for their use in the synthesis of zeolites. The decisive parameters are polarity (hydrophobicity/hydrophilicity), size, charge, and shape of the OSDA.

5.1.1. Polarity

Since high-silica hydrophobic zeolites are synthesized in water with the aid of OSDAs, the OSDA must be moderately hydrophobic while being water soluble and have only a weak tendency to form complexes with the solvent. On this basis, organic molecules with quaternary ammonium are suitable candidates. Zones et al.^[87] have discussed the effect of the carbon to nitrogen ratio (C/N^+) of organic molecules on the crystallization of zeolites. They concluded that a C/N^+ between 11 and 16 is optimum for the synthesis of high-silica porous materials, and moderately hydrophobic OSDAs are the most suitable. To study the polarity effect, Zones et al. have determined the distribution of organic molecules in an aqueous solution and an organic chloroform phase. The molecules that distribute well in both phases have an adequate polarity to function as good OSDAs.^[88]

To make extra-large-pore zeolites, it may seem logical to use large OSDAs. However, it should be taken into account that as the size of the organic molecule increases, its hydrophobicity also increases (polarity decreases), something which limits its solubility in aqueous media and its ability to form solvated cations. To be soluble in water, a certain polarity (adequate C/N^+) is needed. In addition to quaternary ammonium, other species that can also be used as OSDAs are macrocyclic ethers,^[89] metal complexes, and more recently, quaternary phosphonium ions.^[90,91,146]

5.1.2. Size and Charge

The OSDA plays an important role in zeolite synthesis by pore filling and for charge balance. The total guest volume must be smaller than or, at most, equal to the free volume of the host framework. Furthermore, the total positive charge carried by all the SDAs must compensate the negative charge of the framework, at least when the synthesis is performed in media containing OH^- ions.

It is possible to define the target zeolite framework so that guest volume will be fixed. Clearly, an OSDA with a large size-to-charge ratio, will introduce a small number of charges and thus control the charge of the framework. This principle was used first by Barrer and Denny,^[82] Aiello and Barrer,^[83]

and Kerr,^[84] who found that, by partially introducing TMA^+ ions ($TMA = \text{tetramethylammonium ion}$) instead of alkali-metal cations into the synthesis gels of zeolite A and sodalite it was possible to increase the Si/Al ratio of the framework, without changing the structure of the zeolite. They recognized that TMA^+ ions with a larger size/charge ratio than alkali-metal cations dictated a lower incorporation of Al atoms into the framework. This effect can be generalized as by controlling the size/charge ratio of the OSDA it is possible to control the T^{IV}/T^{III} framework ratio, and to synthesize high-silica or even pure-silica zeolites.^[92-95,142] Since the synthesized pure-silica zeolites have to be electrically neutral, the charge of the OSDA must be compensated by the presence of framework defects ($Si-O^-$) when the synthesis is carried out in OH^- ion containing media. However, when using F^- ions as a mineralizing agent, the charge of the SDA can be compensated by F^- ions encapsulated in the secondary building units, and even by F^- ions present in the main channels. This situation implies that in F^- based synthesis, no framework defects are required to compensate the charge of the OSDA and consequently highly hydrophobic, pure-silica zeolites will be produced. This relationship can be seen in Figure 2 in the "framework charge density" triangle.

It can be summarized that, for a specific zeolite, the final framework charge density is determined by a compromise between the size/charge ratio of the OSDA, and the presence of F^- and T^{III} (T^{II}) atoms. Each OSDA has a fixed size/charge ratio, thus the total guest volume is determined by the number of guest molecules that will correspond to the framework charge density. This effect was pointed out by Burton and Zones,^[96,97] who showed that, when the same OSDA was used, the framework density decreases (or the pore volume increases) when increasing the level of T^{III} framework substitution (Figure 3). The relationship between framework density, guest volume, and level of T^{III} framework substitution can be seen in Figure 2 arrow 5.

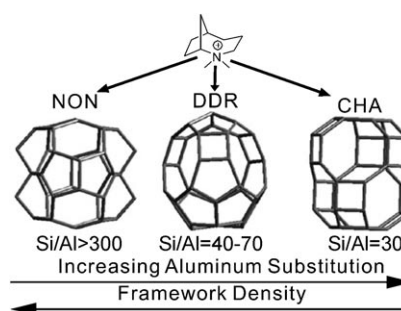


Figure 3. Changes in phase selectivity observed with varying Si/Al ratio for a polycyclic SDA molecule examined in Ref. [96].

5.1.3. Size and Shape

Intuitively, it is expected that the size and shape of an organic guest will affect the phase selectivity. Davis and Lobo^[98] suggested that the OSDA can play three different roles: 1) space-filling agents, 2) structure-directing agents, 3) templates. There are two cases of the OSDA acting as a

true structure-directing agent: the *N,N,N*-trimethylammonium derivative of 1-adamantanamine in the synthesis of SSZ-24^[99] and 1,4,7,10,13,16-hexaoxacyclooctane ([18]crown-6) in the synthesis of hexagonal Faujasite (EMT).^[100] Additionally, they that there may only be one example in all the literature on zeolites and molecular sieves that qualifies as a true templating. A specific $C_{18}H_{36}N_3^+$ triquatary amine (triquat) is necessary for the synthesis of ZSM-18 owing to its symmetry being a perfect match.^[81] The fact that, ZSM-5 and ZSM-48 can be synthesized with at least 22 and 13 different organic molecules, respectively, indicates that these OSDAs are not acting as a structure directing agents but rather as space fillers. As mentioned in Section 5.1.1, organic molecules that are effective for crystallizing high-silica phases tend to have a C/N^+ ratio between 11 and 16. Furthermore, the most selective SDAs are those composed of more than 16 atoms, have two or three charges per molecule, and have very low flexibility.^[87] When the SDA is increased to a certain dimension, the product formed changes from a clathrasil to microporous molecular sieve (Figure 4 and Figure 5).^[101–104]

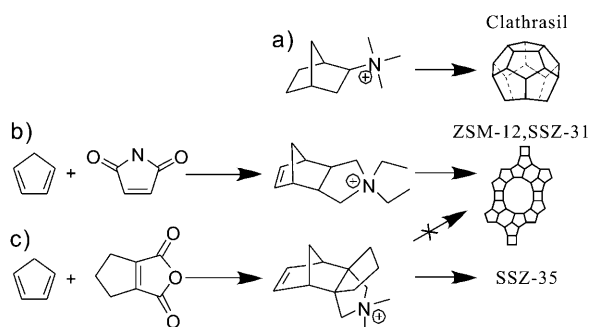


Figure 4. Three guest molecules generated by extensions of the Diels–Alder reaction and the types of zeolites generated as spatial features of the guests change. a) The norbornyl derivative is still small enough to generate cage-centered clathrate structures, such as nonasil (NON). b) The tricyclic derivatives with a long, central axis produces one-dimensional, large-pore zeolites, such as ZSM-12 (MTW structure) and SSZ-31. c) The pseudo-propellane guest leads away from one-dimensional large-pore zeolites and generates zeolites with cavities such as SSZ-35. Taken from Ref. [101].

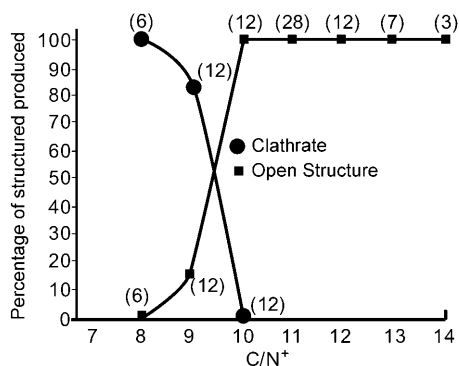


Figure 5. Clathrate versus open framework formation. Numbers in parentheses indicate how many results contribute to this graph point. Taken from Ref. [104].

To discover new zeolites, more complex OSDAs have been synthesized by means of Diels–Alder,^[101,105,106] Beckman rearrangement,^[107] and other multistep synthesis reactions among which the reduction of alkyl nitriles and the amination of acyl halides have allowed the synthesis of the extra-large-pore 14R SSZ-53 (SFH) and SSZ-59 (SFN), respectively.^[47]

5.1.4. The Flexibility of the OSDA and the Possibility of Self-Assembly

A true template is a molecule that can fit perfectly within the framework and maximize Van der Waals interactions with the (in the case of zeolites, inorganic) walls. Thus by considering the OSDAs as isolated molecules, researchers have synthesized bigger and more rigid OSDAs and used them to obtain large- and extra-large-pore zeolites. However, this direction was limited by the organic synthesis and the requirement of size, shape, and polarity. So it is reasonable to consider making larger OSDAs by self-assembling smaller organic molecules with the adequate polarity to form the corresponding “dimer”. This approach requires that the supramolecular OSDA, formed by the self-assembly of the two moieties, remains stable under synthesis conditions.

5.1.4.1. π – π Interactions between Rigid OSDAs

An example of the formation of large and rigid OSDAs by supramolecular self-assembly of two smaller molecules in the synthesis gel has been reported for the preparation of the pure silica LTA (ITQ-29).^[95] In this case it is not possible to make use of hydrogen-bonding interactions to achieve the supramolecular self-assembly because the synthesis is carried out in aqueous media, and thus other types of interactions need to be exploited, such as for instance π – π -type interactions, to assemble the two starting organic molecules (Figure 6). Two OSDA cation molecules self-assemble to a dimer during the gel formation, and fill the spherical α cage of the LTA to direct the synthesis towards the production of the high-silica zeolite A (Figure 6, see also Figure 2 arrow 3).

In addition to π – π -type interactions, hydrophobic interactions can also be a driving force for supramolecular self-

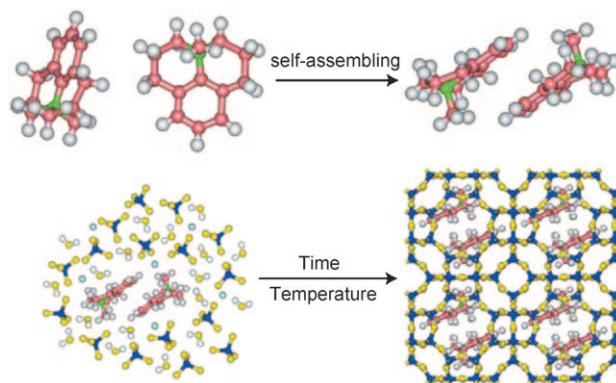


Figure 6. Formation of the LTA structure through the supramolecular self-assembly of the OSDA molecules. Taken from Ref. [95].

assembling OSDAs in zeolite synthesis, as will be shown below.

5.1.4.2. Hydrophobic Interactions between Flexible Linear OSDAs

One of the most fruitful OSDAs is hexamethonium, which can be used to synthesize EU-1,^[108] ZSM-48,^[109] ITQ-13,^[110] ITQ-17,^[111] IM-10,^[112] ITQ-22,^[113] ITQ-24,^[114] EMM-3,^[115] and ITQ-33.^[52] Clearly, the linear and flexible hexamethonium should pack in different ways to fill up the channel of various zeolites. Unfortunately, owing to the lack of single-crystal structure data (except ITQ-13) the packing of the OSDA in the channels is not known exactly. Hopefully, computer simulation will help us to understand how the OSDA molecules in the zeolite cavities interact. Unlike surfactants, they do not come together forming a micelle, also they are not packed like rigid OSDAs in large-pore- and extra-large-pore zeolites, such as in SSZ-53^[47] and SSZ-59.^[47] Thus, to properly fill the pores they must interact through hydrophobic interactions. Apparently, linear and flexible OSDAs favor interactions with each other in extra-large-pore zeolites (Figure 2 arrow 4). Moreover, the gel concentration will greatly affect the packing model, and more concentrated gels should favor this type of interaction.

5.2. Synthesis under Concentrated and Diluted Conditions

Zeolite synthesis is usually performed in an aqueous medium that contains dissolved reagents and solid species suspended in solution. Following on from conventional hydrothermal synthesis, several improved methods have been developed. For instance, the dry-gel-conversion^[116] synthesis methods, in which the solid species are kept separated from the aqueous phase, and vapor-phase transportation (VPT),^[117] or steam-assisted conversion (SAC),^[118] have been used to synthesize various zeolites.^[119–121] The combination of F⁻ ions with highly concentrated gels has allowed a number of low-framework density zeolites to be prepared in their purely siliceous form.^[122,123] Different from the dry-gel method, in this later method the gel is not separated from the aqueous phase and the H₂O/SiO₂ ratios are lower than 10.

Fluoride was first applied in molecular-sieve synthesis by Flanigen and Patton,^[124] and it was later widely studied by Guth et al.^[125] The use of F⁻ ions as a mineralizer allows the synthesis to be performed at lower pH values than in media containing OH⁻ ions, and opens new possibilities for zeolite synthesis. For instance, compared to OH⁻ ions, the presence of fluoride produces high-silica zeolites with fewer of the defects that arise from the charge-balance effect (Figure 2). The use of F⁻ ions also allows framework cations that are insoluble in alkali medium to be incorporated. Furthermore, OSDAs that are not stable under higher pH values and temperatures can be used when working in F⁻ ion containing media. Finally, F⁻ ions tend to occupy small cages and stabilize them, especially D4R. The relationship can be seen in Figure 2 arrow 8.

The effect of the H₂O/SiO₂ ratio on synthesis products was studied by several authors, and Cambor et al.^[126,127] have reviewed the synthesis of a number of high-silica zeolites synthesized from concentrated gels in fluoride media. It was shown (Figure 7) that the synthesis under different H₂O/SiO₂

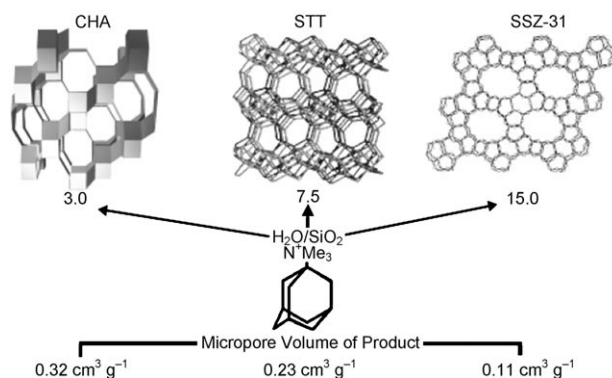


Figure 7. Synthesis under different H₂O/SiO₂ ratios can produce different zeolites. Taken from Ref. [103].

ratios in the presence of the same type of OSDA can produce different zeolites and, in general, lower H₂O/SiO₂ ratios in the synthesis gel produce zeolites with lower framework densities. Lower H₂O/SiO₂ ratios should also increase the rate of nucleation and facilitate the incorporation of F⁻, and OSDAs with the corresponding effect of favoring the synthesis of structures with larger micropore volumes.

By studying the effect of gel concentration, Zones et al.^[105] have found that the highest F⁻ ion and OSDA uptakes occur at the lowest H₂O/SiO₂ ratio, together with a transformation from more dense to more open phases. By working with a series of piperidinium derivatives as OSDAs in concentrated and diluted F⁻ ion media, it was found,^[104] that the products with the highest framework density (either clathrasil or the zeolite MTW with a 1D channel system and 19.3 T atoms per 1000 Å³) are mostly found in diluted media, whereas as the previously reported,^[126,127] “default structure” zeolite Beta (15.1 T atoms per 1000 Å³) is obtained in concentrated media. The statistical work shown in Figure 8 clearly demonstrates

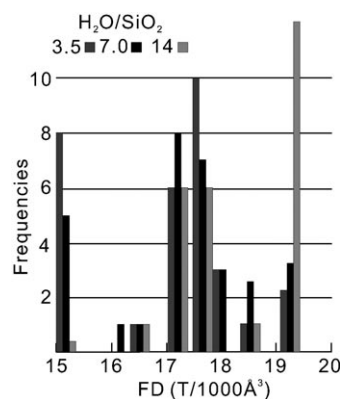


Figure 8. Frequency of framework-density types versus synthesis concentration. Taken from Ref. [104].

that synthesis in concentrated-media favors the formation of low framework-density zeolites and vice versa.

In summary, for producing zeolites with a lower framework density (or larger micropore volume), the use of larger and rigid OSDAs with the correct polarity, or the use of smaller rigid or flexible OSDA molecules that can undergo self-assembly or make compatible interactions is required. The use of concentrated gels can increase the chance of synthesizing zeolites with lower framework density, which is a feasible strategy towards the synthesis of extra-large-pore zeolites with multidimensional system of channels.

5.3. Isomorphous Substitution: The Heteroatom Effect

5.3.1. Influence of T^{III} and T^{II} Atoms

Different trivalent and divalent metals have been introduced in larger or smaller amounts in various zeolite frameworks. It is clear that the introduction of T^{III} or T^{II} elements in framework positions will generate negative charges that will have to be balanced by cations. Thus, in fluoride media, the sum of charges derived from the isomorphous substitution together with the F^- ion present in channels and/or within secondary building units, will determine the amount of OSDA within the pores and, as a consequence, it will have an impact on the micropore volume of the synthesized zeolite. On the other hand, elements other than Si will have different T–O bond lengths and T–O–T angles to Si and thus be able to stabilize other secondary building units and induce the formation of new structures. For instance in the case of Ga, an extra-large-pore gallosilicate ECR-34 (ETR) has been synthesized by Strohmaier and Vaughan^[48] using Na^+ , K^+ , and TEA^+ ions as the SDA. This zeolite with 18R pores has no aluminosilicate analogue yet, and it is built from SBUs never seen in aluminosilicate frameworks. However, another gallosilicate CGS is synthesized with K^+ ions,^[128] showing that the formation of that particular SBU is a result of the structure-directing effect of K^+ ions and Ga.

Another T^{III} element, such as B, can form B–O–Si angles in zeolites which are, on average, smaller than Si–O–Si, Al–O–Si, or Ga–O–Si angles. During the past decade, a series of new zeolite structures has been successfully synthesized in the form of borosilicates.^[47, 129–135]

The divalent beryllium cation can be tetrahedrally coordinate and there are several beryllium-containing natural zeolites, such as Lovdarite and Nabesite, that have 3R in their structures. In addition, two 3R-containing zeolites, OSB-1 (OSO) and OSB-2 (OBW) have been prepared with beryllium.^[46] OSB-1 has 3D arrangement of $14 \times 8 \times 8R$ pores and with a very low framework density (see Figure 1b). Davis^[5] addressed the challenge of building zeolite frameworks based on 3R, and has developed extensive work on environmentally friendly Zn zeolites since postulating that Zn can promote the formation of 3R. Indeed three zincosilicates (VPI-7 (VSV),^[136] VPI-9(VNI),^[137] and RUB-17 (RSN)^[138]) have been synthesized that have 3-membered rings, though in these cases no extra-large pores are present.

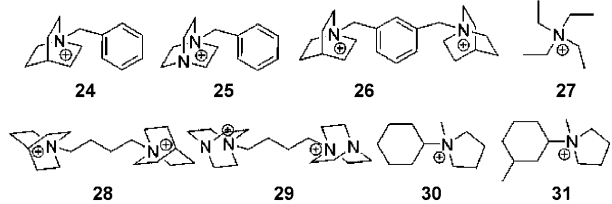
It appears that the introduction of T^{III} and T^{II} elements can direct the formation of new zeolites, and more specifically

of zeolites with 3R- and 4R-containing frameworks. However, in these cases framework charges are also introduced which also influence the zeolite synthesis and, consequently, it is difficult to separate both effects. Based on the above factors we thought of expanding the range of T–O–T angles in zeolites without introducing framework charges and proposed that this could be done by synthesizing germanosilicates.

5.3.2. Germanium as a Key Atom to Control D4R

A series of germanates with D4R structures has been reported.^[139, 140] It appeared then that the presence of D4R is quite common in germanates. In the case of pure silicious structures, the average Si–O–Si bond angle is about 148° . However in a pure-silica zeolite structure the D4R interatomic bond angles tend to be smaller because of the 90° Si–Si–Si angle of the D4R cube. The presence of Ge in the zeolite synthesis could increase the possibility of forming D4R-containing frameworks because of the smaller Ge–O–Ge or Si–O–Ge angles compared to Si–O–Si angle. This feature, together with the fact that F^- ion can also stabilize the formation of D4R, inspired us to introduce Ge during the synthesis of zeolites in concentrated gels and with F^- ions as a mobilizing agent. Theoretical energy calculations showed that the introduction of up to three Ge atoms in the D4R unit stabilizes this secondary building unit.^[141a] Furthermore, when small amounts of Ge were introduced during the synthesis of ITQ-7^[141b] (a pure silica zeolite with D4R^[141c]), the crystallization time decreased from seven days for the pure silica to less than one day for a sample with Si/Ge = 20. Interestingly, and as predicted by theory, Ge was preferentially occupying positions at the D4R units.^[141c] Furthermore, a strong directing effect of Ge towards structures containing D4R, also in the absence of F^- , has been demonstrated by performing the synthesis of the polymorph C of Beta (BEC) with a large variety of OSDAs. When the synthesis was carried out only with SiO_2 and in F^- media, different structures were obtained depending on the OSDAs. However, when Ge was introduced only the BEC structure was obtained regardless of the OSDA used (see Table 4).^[111] In fact, the BEC structure has been obtained before as a germanate within a mixture of FOS-5 (BEC) and ASU-9,^[140] though the structure-directing role of Ge was not reported. In our case, pure BEC could be obtained as a silicogermanate with a large variety of OSDAs thus demonstrating the directing effect of Ge towards structures with D4R, and we could determine that the location of Ge in the framework corresponds to that predicted by theoretical calculations.^[141a] Recently, the pure-silica BEC structure has been synthesized with an optimized OSDA that strongly stabilizes this structure.^[142]

In summary, the introduction of Be, Zn, and Ge can lead to structures with 3R and 4R. Since 3R and 4R are necessary for zeolites with low framework density, the introduction of these heteroatoms will facilitate the synthesis of extra-large-pore zeolites

Table 4: Synthesis conditions and zeolitic structures obtained by using different SDAs with and without germanium in the crystallization gel (taken from Ref. [111]).


SDA	H ₂ O [wt%]	Si/Ge	T [°C]	t [h]	Ge zeolite	SiO ₂ zeolite
24	8	1–10	150	15–120	polymorph C	ITQ-4
25	8–24	0.5–30	135–175	15–120	polymorph C	ITQ-4
26	8	5	150	16–96	polymorph C	Beta
27	7.5	2	140	96	polymorph C	Beta
28	7.5–15	2–10	175	24–96	polymorph C	Beta, ZSM-12
29	15	2–20	175	24–96	polymorph C	ZSM-12
30	7.25	5	135–175	15–96	polymorph C	ZSM-12
31	7.25	5	135–175	15–96	polymorph C	Beta

6. Synthesis of Extra-Large-Pore Zeolites

Of the 191 frameworks identified by the Structure Commission of the International Zeolite Association only 10 correspond to extra-large-pore zeolites. In addition to these 10, there are other structures containing extra-large pores in their frameworks, including ITQ-33, ITQ-37, and ITQ-40. In Table 5 the structures and OSDAs used for the synthesis are listed.

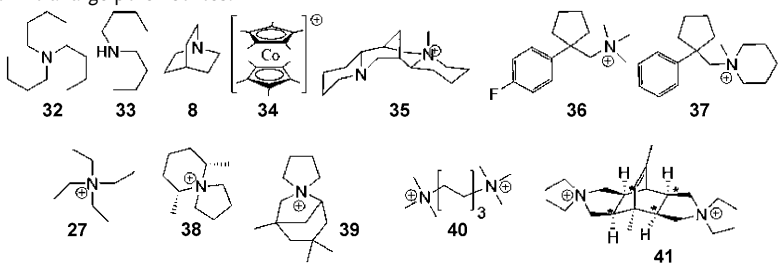
Taking into account all the conclusions on the influence of the synthesis parameters described above, the following strategies have been applied for the synthesis of extra-large-pore zeolites:

1. Large and rigid three-dimensional OSDAs with the required polarity to produce materials with larger micropore volume and a multidimensional system of channels.
2. Concentrated gels and fluoride media to increase the probabilities for producing structures with lower framework density.
3. Synthesis of frameworks containing 3R and 4R, and more specifically D4R, to give structures with low framework density.
4. High-throughput (HT) synthesis techniques to explore a wide synthesis space.

Corma et al. selected the OSDA **35** (Table 5) for the synthesis of a new 3D large-pore zeolite ITQ-21,^[143] which accomplished strategy (1) and was already known to

be adequate for the synthesis of a 1D 14R channel zeolite CIT-5.^[45] By using methylsparteinium (**35**) and working with concentrated gels in fluoride media and using Si and Ge as T^{IV}, a factorial design for defining the synthesis of ITQ-21 was established. ITQ-21 has a framework density of 13.5 T/1000 Å³.^[143b] A sample with a Si/Ge ratio of 20 could be prepared. ITQ-21 zeolite contains D4R units and Ge preferentially occupies this unit until three Ge atoms have been introduced into each D4R. Then, in agreement with theoretical predictions, Ge starts to occupy vicinal positions to the D4R.^[143b] This structure is of much interest since it is formed by three 12R (0.73 nm in diameter) linear channels that cross perpendicularly. In some ways it is reminiscent of the channel structure of zeolite A (LTA), but with the distinct difference that the channels in ITQ-21 are 12R instead of 8R.

The successful synthesis of a D4R-containing zeolite with a very large micropore volume has motivated further synthesis work using new OSDAs. By working with rigid and even bulkier OSDAs (such as **39** in Table 5) in concentrated

Table 5: Extra-large-pore zeolites.


Structure code	Material	Year	Channel dimension	Framework atoms	Framework density [T atoms nm ⁻³]	Template	Ref.
VFI	VPI-5	1988	1D 18 R	Al, P	14.5	32, 33	[10]
AET	AIPO-8	1990	1D 14 R	Al, P	18.2	33	[11]
-CLO	Cloverite	1991	3D 20 R	Ga, P	11.1	8	[13]
DON	UTD-1	1996	1D 14 R	Si	17.1	34	[44]
CFI	CIT-5	1997	1D 14 R	Si	16.8	35	[45]
SFH	SSZ-53	2003	1D 14 R	B, Si	16.5	36 ^[a]	[47]
SFN	SSZ-59	2003	1D 14 R	B, Si	16.6	37 ^[a]	[47]
OSO	OSB-1	2001	3D 14 × 8 × 8 R	Be, Si	13.3	K ⁺	[46]
ETR	ECR-34	2003	3D 18 × 8 × 8 R	Ga(Al), Si	15.4	27 and Na ⁺ , K ⁺	[48]
UTL	IM-12 or ITQ-15	2004	2D 14 × 12 R	Ge, Si	15.6	38 (for IM-12), 39 (for ITQ-15)	[50, 51]
-	ITQ-33	2006	3D 18 × 10 × 10 R	Ge, Si	12.3 ^[b]	40	[52]
-	ITQ-37	2009	3D 30 R	Ge, Si	10.3 ^[c]	41	[158]

[a] Only one example with this SDA. [b] Taken from Ref. [52]. [c] Taken from Ref. [158].

gels, fluoride media, and Ge, a new extra-large-pore zeolite (ITQ-15) with 2D $14 \times 12R$ channels was prepared,^[49,50] as well as some new extra-large-pore zeolites with 3D pore systems, including ITQ-37, the first 3D mesoporous silicate zeolite with 30R channels. It has the lowest framework density ($10.3 \text{ T atoms}/1000 \text{ \AA}^3$) of all reported zeolites, and its structure and properties will be described in Section 7. This structure contains 3R and D4R units demonstrating again the positive effects of Ge and large rigid OSDAs for the synthesis of extra-large-pore zeolites.

In 1995, Strohmaier and Vaughan^[144] reported the gallosilicate zeolite ECR-34 with a $18 \times 8 \times 8R$ channel system.^[48] Interestingly, the SDAs were Na^+ , K^+ , and TEA^+ ions. Large OSDAs were not required because the high framework charge (Si/Ga about 3) requires a large amount of cations and water enclosed within the pores, generating a large micropore volume. This work suggested that it could be possible to produce low framework-density materials using smaller and flexible OSDAs. Along this line, Corma et al. opened a synthesis direction working with Ge and using the smaller and flexible trimethonium, tetramethonium, and hexamethonium dications as OSDAs (see Figure 9). With this type of organic

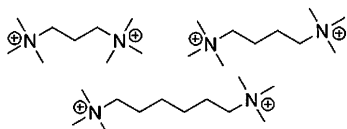


Figure 9. Three smaller and flexible dicationic OSDAs.

species, a large number of positive charges were introduced to compensate the presence of a large number of F^- ions in D4R cages, and in addition the organic species were able to fill the pores.

While trimethonium could produce octadecasil (AST) and nonasil in OH^- and F^- media, respectively, hexamethonium produced a zeolite structure with a D4R-containing structure, namely ITQ-24^[144] with 12R, when working in OH^- media with Ge and B, and ITQ-22 with $12 \times 10 \times 8R$ pores when working in OH^- media with Si and Ge.

Hexamethonium is a dicationic template which generated, when working with HT synthesis techniques under unusual synthesis conditions ($\text{OH}^-/\text{T}^{\text{IV}} = 0.1$ and $\text{H}_2\text{O}/\text{T}^{\text{IV}} = 5$, $\text{T}^{\text{IV}}/\text{T}^{\text{III}} = 20$), a new zeolite named ITQ-33.^[52] Besides this new material, other known structures, such as EU-1, SSZ-31, ITQ-22, and ITQ-24 were also obtained. Furthermore, by means of an optimized HT experimental design, ITQ-33 was crystallized as a pure silicogermanate material and the structure was solved (Figure 10).^[52] This material has 3R and D4R units in the structure, and exhibits a unique topology with an extra-large-pore channel with circular openings of 18R (diameter 12.2 \AA) along the *c*-axis interconnected by a two dimensional system of 10R channels. ITQ-33 was the silicate zeolite with the lowest framework density at that time ($12.3 \text{ T}/1000 \text{ \AA}^3$). However the most interesting structural feature is the combination of 18R and 10R interconnected channels that showed excellent and unique gas oil cracking properties to maximize diesel and olefin production (see Section 9).^[52,145]

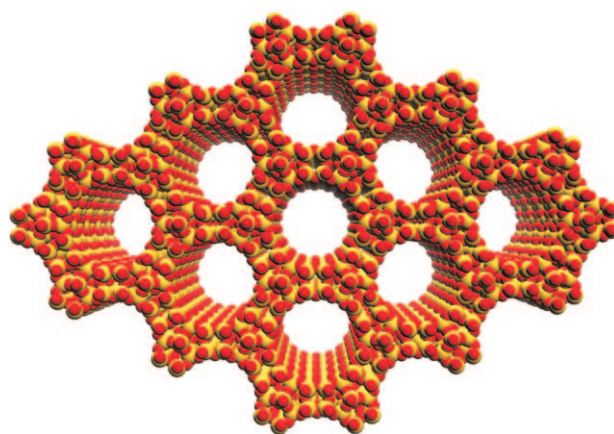


Figure 10. View along the *c*-axis showing the 18R channel in the structure of ITQ-33.

It should be noticed that the synthesis of extra-large-pore zeolites are not restricted to the use of organoammonium templates, other templates, such as phosphonium ions which do not suffer from the Hoffman decomposition in basic environment can also be used. With the phosphonium templates three new structures ITQ-26 (IWS),^[90] ITQ-27 (IWV),^[91] and ITQ-34 (ITR)^[146] have been obtained.

7. Synthesis of a Mesoporous Chiral Zeolite

The synthesis of mesoporous materials with long-range order and different pore dimensions and topologies has opened many potential applications in, for example, catalysis,^[147] electronics,^[148] controlled delivery of chemicals,^[149,150] adsorption,^[151] and light harvesting.^[152] Representative examples of the ordered mesoporous materials are the M41S series (e.g., MCM-41 and MCM-48^[147,149,152]) from Mobil and the SBA family from Santa Barbara University.^[148–150] These materials have no short-range order and resemble amorphous silicates with uniform pores rather than crystalline molecular sieves in terms of the local structure, bonding, and physico-chemical properties.^[153,154] There have been many research efforts aimed at producing mesoporous materials with crystalline walls. Unfortunately, none of these efforts has been successful to date. Even though mesoporous materials with walls containing zeolite secondary building units of the type found in zeolites could be prepared,^[155–157] short-range order has not been observed.

To produce inorganic mesoporous crystalline materials, one option could be to start from crystalline microporous molecular sieves and try to increase their pore diameters. As shown in Section 2, germanates SU-M and SU-MB and JLG-12 with 30R channels and pore openings over 2.0 nm can be considered as mesoporous crystalline materials. The discovery of these mesoporous crystalline materials, although they are not stable upon removing the template, and they are not zeolites in the strict sense, indicates that it could be possible to synthesize mesoporous zeolites.

Our efforts to obtain extra-large-pore zeolites following the synthesis strategies using large, rigid three-dimensional

OSDAs, concentrated gels, fluoride media, and Ge, gave ITQ-37, the first mesoporous material with an interrupted zeolite framework.^[158] ITQ-37 was synthesized using the bulky diammonium ion **41**, which contains chiral centers, as the OSDA (Table 5). ITQ-37 has a very open framework consisting of one unique lau cage^[4²6⁴] and two unique D4R units. The structure has 30R pores (2.2 × 0.7 nm diameter) which result in a large accessible volume (see Figure 11). The

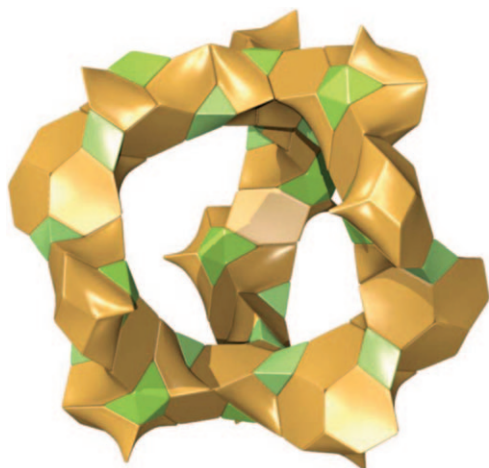


Figure 11. Tiling of the srs net for a large cavity defined by three 30R channels. Taken from Ref. [158].

BET surface area of the silicogermanate ITQ-37 of 690 m² g⁻¹, allows a value of 900 m² g⁻¹ to be extrapolated for the pure silica polymorph and a micropore volume of 0.38 cm³ g⁻¹. Interestingly, ITQ-37 has the lowest framework density (10.3 T atoms per 1000 Å³) of all four-coordinate crystalline oxide framework materials. It can be calcined at 600 °C while maintaining the structure. Since ITQ-37 was synthesized with Al, it has Brønsted acidity and can be used as a crystalline mesoporous catalyst^[159] (see Section 9).

ITQ-37 is also a chiral zeolite in which the framework represents the SrSi₂ (srs) minimal net and forms two unique cavities, each of which is connected to three other cavities to form a gyroidal channel system.^[158] These cavities comprise the enantiomorphous srs net of the framework.

The discovery of ITQ-37 shows that zeolites can reach pore dimensions on the order of the mesoporous scale, and provides new insight towards targeting chiral crystalline frameworks with extra-large pores. However a question arises as to how large a pore size is possible? This question was addressed by Davis^[5] who discussed that for zeolites synthesized in water it is unlikely that materials can be synthesized when the density of the crystals is less than that of water. However he also pointed out that “the bound on void volume may only apply to those preparations not involving thick gels” as has been in the case of the extra-large-pore ITQ materials.

8. Germanium-Containing Zeolites: Limitations and Potential Solutions

To date a large number of germanosilicate structures have been synthesized. However, there are two main drawbacks for the practical use of Ge containing zeolites, the hydrothermal stability and the price of germanium. In fact, hydrothermal and thermal stability is not a limitation for materials with a Si/Ge ratio above 20, or even lower than 20 for samples with higher framework density. Zeolites should be synthesized with Si/Ge ratios over 200 to meet economic considerations. However, when samples with Si/Ge ratios above 20 are synthesized, a large part of the residual Ge can be recovered by a post synthesis treatment.^[160] Furthermore, the synthesis procedures have been further developed in our group so that the same structures can be obtained but free of Ge. Theoretical energy minimization methods are considered to find OSDAs that could better stabilize the structures, together with a search for optimum synthesis conditions. Table 6 shows the germanosilicate zeolites of the ITQ-family and their respective minimum Ge contents achieved to date. The results show that there is still a possibility that by combining the use of optimized OSDAs, optimized synthesis conditions, and postsynthesis methods, the Ge/Si ratio in germanosilicates could be significantly reduced, even to zero.

9. Adsorption and Catalysis

Extra-large-pore zeolites have been highly desired for a long time^[3] for their potential ability to process bulkier molecules. In the case of, VPI-5 and AlPO₄-8, owing to the absence of potential active sites, their use as catalysts could only be attempted after isomorphous substitutions by other elements, such as, Ti, Co, Cu, Mg, V, in framework positions to generate acid, basic, or redox-active sites.^[161–168] In the case of Cloverite, the catalysis work has been concentrated on the acidity of the terminal P-OH groups.^[169–173] Unfortunately, the low thermal stability of this material greatly restricts its applications as a catalyst.

Also silica-based zeolites with extra-large pores including CIT-5, UTD-1, SSZ-53, and SSZ-59 have been considered. Though all of them have a 1D 14R channel system, the pore shapes and effective pore diameters for catalytic reactions are quite different and these differences should affect their adsorption and catalytic properties.

Chen and Zones^[174,175] have measured the adsorption properties of these extra-large-pore zeolites (see Table 7). It can be seen that all those zeolites can easily adsorb small sorbates, such as *n*-hexane, cyclohexane, and 2,2-dimethylbutane. But for more bulkier sorbates, such as 1,3,5-triisopropylbenzene with a kinetic diameter of about 0.85 nm, only the 14R zeolites UTD-1, SSZ-53, and SSZ-59 with pore diameters over 0.80 nm, the 18R aluminophosphate VPI-5, and the 3D 12R NaY zeolite are able to adsorb significant amounts. They also studied the catalytic performance for isomerization and disproportionation of 1,3-diisopropylbenzene over 12R and 14R zeolites (see Table 8). It can be seen there that when the pore size decreases, more isomerization to 1,4-diisopropyl-

Table 6: Germanosilicate zeolites of the ITQ series, and the minimum Ge content achieved.

Name	Code	Pore system	Si/Ge ratio first reported	Si/Ge ratio minimum achieved	SDA	Ref.
ITQ-1	MWW	2D 10×10R	Ge free		42	[92]
ITQ-3	ITE	2D 8×8R	Ge free		43	[199]
ITQ-4	IFR	1D 12R	Ge free		24	[200]
ITQ-7	ISV	3D 12R	Ge free		39, 43, 44	[141]
ITQ-9	STF	1D 10R	Ge free		43	[201]
ITQ-12	ITW	2D 8×8R	Ge free		45, 46	[202]
ITQ-13	ITH	3D 10×10×9R	Ge free		40	[110]
ITQ-15	UTL	2D 14×12R	Si/Ge=10		39	[49, 50]
ITQ-17	BEC	3D 12×12×12R	Si/Ge=2	Ge free (ITQ-14)	44 R',R=H	[111, 142]
ITQ-21	–	3D 12×12×12R	Si/Ge=20	Si/Ge=40	35	[143]
ITQ-22	IWW	3D 12×10×8R	Si/Ge=20		40, 47	[113]
ITQ-24	IWR	3D 12×10×10R	Si/Ge=5	Ge free (seed)	40, 41	[94, 114]
ITQ-26	IWS	3D 12×12×12R	Si/Ge=4		48	[90]
ITQ-27	IWV	2D 12×12R	Ge free		48	[91]
ITQ-29	LTA	3D 8×8×8R	Ge free		49	[95]
ITQ-32	IHW	2D 8×8R	Ge free		50, 51	[203]
ITQ-33	–	3D 18×10×10R	Si/Ge=2		40	[52]
ITQ-34	ITR	3D 10×10×9R	Si/Ge=10		52	[146]
ITQ-37	–	3D 30R	Si/Ge=1		41	[158]

Table 7: Adsorption property of various zeolites, taken from Ref. [175].

Zeolite	Pore Size [Å]	Pore system	Adsorption capacity [mL g ⁻¹]			
			<i>n</i> -hexane ($\sigma=4.4$ Å) ^[a]	cyclohexane ($\sigma=6.0$ Å) ^[a]	2,2-dimethyl- butane ($\sigma=6.2$ Å) ^[a]	1,3,5-triisopropylbenzene ($\sigma=8.5$ Å) ^[a]
NaY	7.3	12R, 3D	0.28	0.25	0.25	0.18
SSZ-24	7.3	12R, 1D	0.10	0.11	0.13	0.01
CIT-5	7.5×7.2	14R, 1D	0.09	0.09	0.09	0.041
UTD-1	8.2×8.1	14R, 1D	0.12	0.11	0.12	0.11
SSZ-53	8.7×6.4	14R, 1D	0.13	0.10	0.12	0.13
SSZ-59	8.5×6.4	14R, 1D	0.16	0.13	0.12	0.11
VPI-5	12.1	18R, 1D	0.20	0.16	0.15	0.12

[a] σ = Kinetic diameter.

benzene and less disproportionation to triisopropylbenzenes occurs. Since no 1,2-diisopropylbenzene was detected, the ratio of 1,4-diisopropylbenzene to triisopropylbenzenes represents the relative selectivity for isomerization versus disproportionation. This ratio increases as the effective pore size of the zeolite decreases, and the results can be explained by transition-state shape selectivity because isomerization proceeds via a monomolecular mechanism while disproportionation involves bulkier bimolecular intermediates. The yield ratio of 1,3,5- to 1,2,4-triisopropylbenzene decreases with decreasing the pore size, because of the product shape selectivity. These results correlate well with the adsorption data of 1,3,5-triisopropylbenzene. It should also be considered

that the diisopropylbenzenes can also be dealkylated during the reaction. Then, if one of the alkyl groups is dealkylated, propylene and cumene should also be detected. When the pore size of the zeolite decreases, the monomeric dealkylation becomes more pronounced, resulting in a higher ratio of cumene to triisopropylbenzenes.

Catalytic test reactions are valuable tools for the characterization of molecular-sieve structures since they provide crucial insights into

the pore architecture and catalytic activity of new molecular-sieve materials whose structures are unknown and/or poorly characterized. Using deuterated *para*-xylene as a reactant, Corma et al.^[176] have found that more than 20% of the *meta*- and *ortho*-xylenes, obtained when using HY zeolite as a catalyst, are formed via a bimolecular mechanism. This route involves, as an intermediate complex, a molecule of trimethylbenzene and another of xylene. The bimolecular process does not occur in the case of ZSM-5.^[176a] *m*-Xylene isomerization and disproportionation have also been used as test reactions^[177] to probe the pore architectures of a series of 1D 12R and 1D 14R pore zeolites. It was found that, unlike multidimensional zeolites with 12R pores that give a *para*/

Table 8: Selectivities of isomerization and disproportionation of 1,3-diisopropylbenzene in various zeolites. Taken from Ref. [175].

Zeolite	Pore Size [Å]	Structure feature	Selectivity [mol %]					Molar Ratio	
			1,4-DIPB ^[a]	TIPBs ^[b]	Cumene	Propylene	1,4-DIPB/ TIPBs	1,3,5-/1,2,4- TIPB	Cumene/ TIPBs
SSZ-53	8.7×6.4	14R, 1D	33.2	14.2	32.5	19.6	2.3	12.8	2.3
SSZ-59	8.5×6.4	14R, 1D	33.4	13.3	31.2	21.4	2.5	12.0	2.3
UTD-1	8.2×8.1	14R, 1D	29.9	20.0	34.3	15.8	1.5	11.7	1.7
CIT-5	7.5×7.2	14R, 1D	39.0	0.0	31.7	29.3	∞	∞	∞
Y	7.3	12R, 3D	33.4	8.8	33.9	23.9	3.8	8.0	3.9
SSZ-24	7.3	12R, 1D	38.4	0.6	31.5	29.3	69.7	0.0	56.9

[a] DIPB: diisopropylbenzene. [b] TIPBs is the isomers of triisopropylbenzene.

ortho (*p/o*) selectivity of > 1, zeolites with 1D pores bounded by 14R or large 12R give a *p/o* only slightly higher than one, as a result of the influence of the bimolecular isomerization mechanism between a xylene and trimethylbenzene.^[176]

The data in Figure 12a show an interesting trend of the initial *p/o* selectivity for the 1D, large-/extra-large-pore catalysts, such as CIT-5, SSZ-24, SSZ-31, and UTD-1. Under the conditions used, these catalysts gave a *p/o* ratio below 1 presumably because of the influence of the *ortho*-selective bimolecular isomerization mechanism.^[176] Although some work demonstrated that the *i/d* (isomerization/disproportionation) ratio cannot be used to accurately distinguish

zeolites of various pore sizes,^[178] in this case it was possible. As presented in Figure 12b, the largest pore zeolites have the lowest selectivity to isomerization, in agreement with previous studies on the reactions of *m*-xylene over zeolitic catalysts.^[179] UTD-1 has the lowest *i/d* value of 0.9. Under the conditions used, the zeolites can be divided into three groups based on their *i/d* ratio: 0–4, for large-pore and extra-large pore zeolites; 8–14 for zeolites with both 12R and smaller pore openings; and > 20 for zeolites with 10R openings. The three exceptions are SSZ-42, Beta, and ZSM-12. The peculiar internal pore architecture of SSZ-42 makes this zeolite quite selective for isomerization. In the case of ZSM-12, although it is a 12R zeolite, the pores are similar in size to those of 10R zeolites.

In addition to xylene, ethylbenzene,^[180,181] and *n*-decane^[181,186] can also be used to probe the effective pore width of acid zeolites. Ernst et al.^[181] have tested the catalytic performance of SSZ-53 for the disproportionation of ethylbenzene, a test reaction that was introduced by Karge et al.,^[182] to distinguish between medium- and large-pore zeolites, based on reaction selectivity.^[183] Figure 13a shows the results of ethylbenzene disproportionation over HSSZ-53. Conversion of around 15% is achieved even at a reaction temperature as low as 150°C. After an induction period the conversion increases and then levels-off into a quasi-stationary state. This behavior is typical for large-pore zeolites. With increasing reaction temperatures, ethylbenzene conversion increases and the induction period shortens or disappears completely. Figure 13b shows the conversion of ethylbenzene and the observed product yields as a function of time-on-stream at a reaction temperature of 200°C. Rather than the ideal ratio 1:1 of benzene:diethylbenzenes, a slightly higher one is found, there is a small diethylbenzene deficit which is a result of the formation of triethylbenzenes. Ernst et al.^[181] also explored the isomerization and hydrocracking of *n*-decane over the bifunctional form of SSZ-53 (0.27Pd/HSSZ-53; Pd content: 0.27 wt%). This reaction has been frequently used for probing the effective pore width of zeolite catalysts. The conversion of *n*-decane and the yields of isomers and hydrocracked products as a function of the reaction temperature are depicted in Figure 14a. As is usually observed, skeletal isomerization of *n*-decane to branched isoalkanes is the sole reaction occurring at very low conversions. Noticeably, a large amount of monobranched isomerization products with side chains longer than methyl groups, that is, 3-, 4-ethyloctane (20 to 30%) and 4-propylheptane (up to ca. 1%) were observed

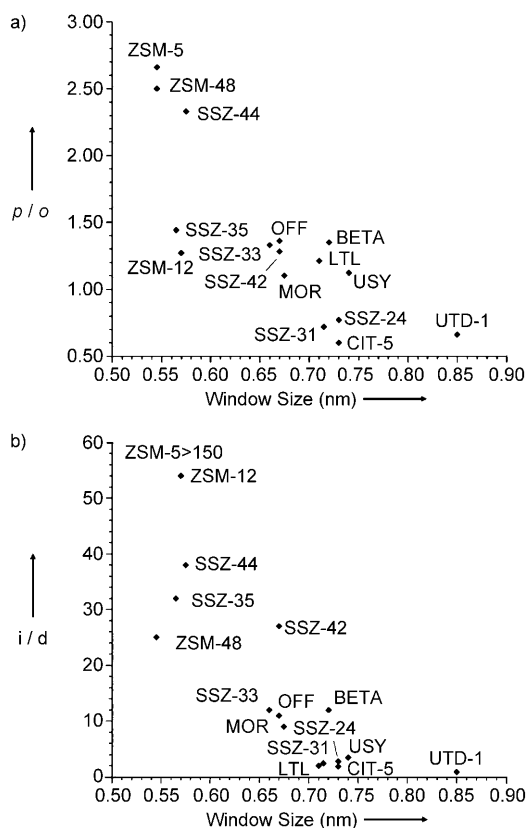


Figure 12. For the conversion of *m*-xylene: a) initial *para/ortho* selectivity versus pore diameter of the largest pore in the zeolite. Conversion = (10 ± 2)%. b) Initial *i/d* selectivity versus pore diameter of the largest pore in the zeolite. Conversion = (10 ± 2)%. Taken from Ref. [177].

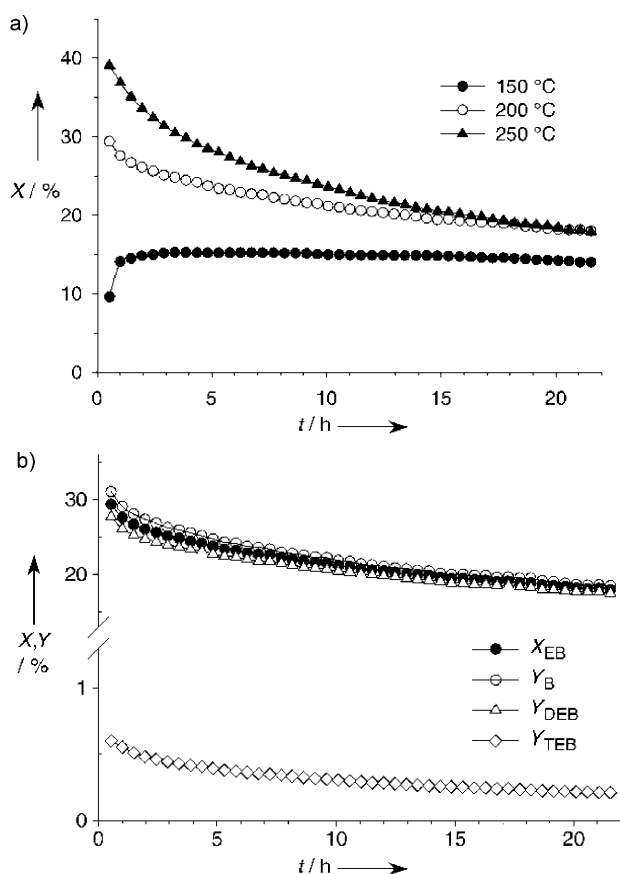


Figure 13. a) Disproportionation of ethylbenzene over HSSZ-53 at different temperatures. b) Conversion and product yields in the disproportionation of ethylbenzene over HSSZ-53 at 200 °C. Taken from Ref. [181].

in isomerization product. This product mix could be advantageous for dewaxing by isomerization. At higher temperature/conversion, hydrocracking also occurs (Figure 14b). The C_1 and C_2 as well as C_8 and C_9 hydrocarbons are absent which suggests that hydrogenolysis, namely hydrocracking at the noble metal, is absent and the predominating reaction mechanism is really a bifunctional one.^[184] From the slightly asymmetric shape of the distribution of the hydrocracked products, it can be deduced that there is a some minor contribution from secondary cracking. Moreover, branched isomers predominate in the C_4 to C_7 fractions, which indicates that hydrocracking starts from highly branched intermediates. This reflects the large space available in the channels of the extra-large-pore zeolite SSZ-53.

There is another test reaction called the spaciousness index (SI).^[185] It documents the ratio of isobutane to n -butane formed during the hydrocracking of a C_{10} -cycloalkane, such as n -butylcyclohexane, over the bifunctional zeolites mentioned above. In this test, the ratio of isobutane to n -butane increases with increasing the zeolite pore size. Burton et al.^[47] have compared the SI index of SSZ-53 and SSZ-59 with other zeolites (Figure 15). According to these results, the effective void sizes of SSZ-53 and SSZ-59 are smaller than the effective diameter of the largest voids in zeolite Y and ZSM-20, but larger than those of 12R zeolites, such as Beta and L.

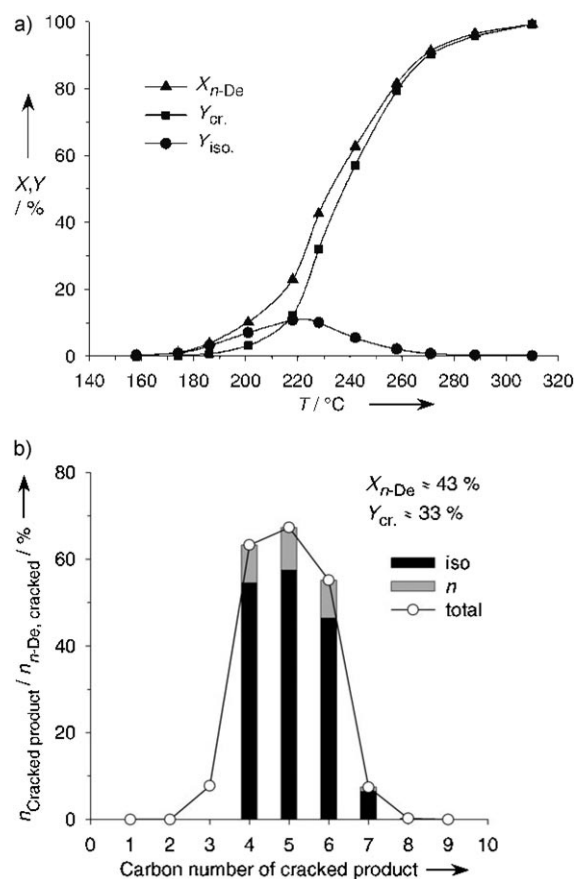


Figure 14. a) Influence of the reaction temperature on the conversion of n -decane (n -De), as well as on the yields of the isomers and hydrocracked products over 0.27Pd/HSSZ-53 as catalyst. b) Distribution of cracked products from n -decane over 0.27Pd/HSSZ-53 at $X_{n-De} \approx 43\%$ and $Y_{cr.} \approx 33\%$. Taken from Ref. [181].

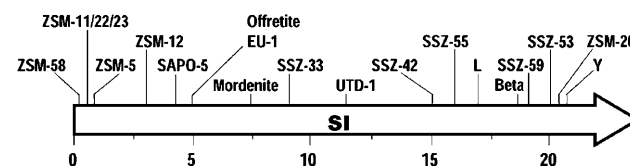


Figure 15. A comparison of the spaciousness indices (SI) of SSZ-53, SSZ-59, and other representative zeolites. Taken from Ref. [47].

Corma et al.^[186] have compared the acid and catalytic performance of 14R channel zeolite CIT-5 and UTD-1 with the 12R channel SSZ-24 zeolite. First the acid sites of the zeolites were characterized. The IR spectrum in the hydroxy region shows that CIT-5 contains two crystallographically distinct bridging hydroxy groups, while UTD-1 has only one (Figure 16a). The relative intensity of the IR band at 1550 cm^{-1} , after pyridine adsorption on the different zeolites, was used to compare the relative number of acid sites. The spectra in Figure 16b show that, in agreement with the framework Si/Al ratio, the number of acid sites decreases in the order SSZ-24 > CIT-5 > UTD-1. Results for the temperature programmed desorption of NH_3 (Figure 16c) show a NH_3 desorption maxima for SSZ-24, CIT-5, and UTD-1 at

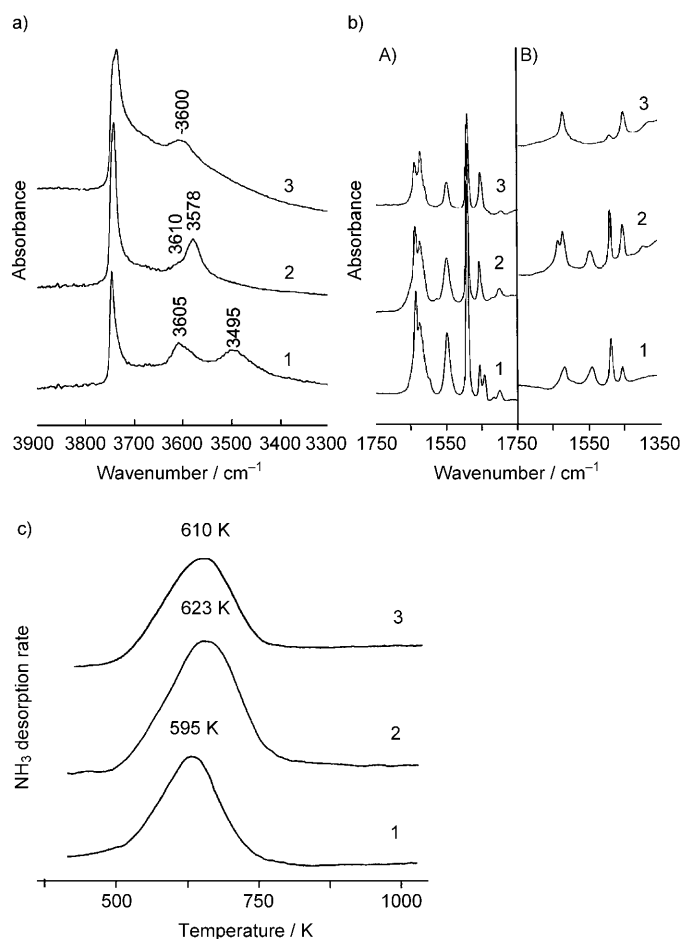


Figure 16. a) Infrared spectra in the OH region of 1) SSZ-24, 2) CIT-5, 3) UTD-1. b) IR spectra of pyridine remaining adsorbed after desorption in vacuum at A) 523 K and B) 673 K. c) Normalized NH_3 temperature programmed desorption of 1) SSZ-24, 2) CIT-5, 3) UTD-1. The spectra are offset for clarity. Taken from Ref. [186].

595, 623, and 610 K, respectively. These temperatures are significantly lower than those of Mordenite (745 K) and ZSM-5 (683 K), but comparable with those of Y-type zeolites (Si/Al = 15–50) (maximum at ca. 623 K), indicating similar acid characteristics of 14R and USY zeolites but weaker acidity than that observed for ZSM-5 and Mordenite.

The cracking activities of the three 14R zeolite samples for a relatively small molecule (*n*-decane), a larger one (1,3,5-triisopropylbenzene), and light vacuum gas oil are presented in Figure 17. The reactivity of *n*-decane, which can easily diffuse through the pore of the three zeolites, should indicate the relative number of acid sites in the zeolites. Indeed, the *n*-decane cracking reactivity (Figure 17a) follows the same order as the acidity measured by pyridine adsorption, SSZ-24 > CIT-5 > UTD-1. For comparison purposes, the 3D 12R zeolite Beta, which has a higher number of acid sites, was also measured, as expected its cracking activity was found to be higher. The larger 1,3,5-triisopropylbenzene molecule with a dynamic diameter of 0.85 nm can pass through the 14R openings, and penetrate into the elliptical pores of UTD-1. However, it is excluded from the pores of CIT-5 and SSZ-24 (see Figure 17b), resulting in a much higher catalytic activity

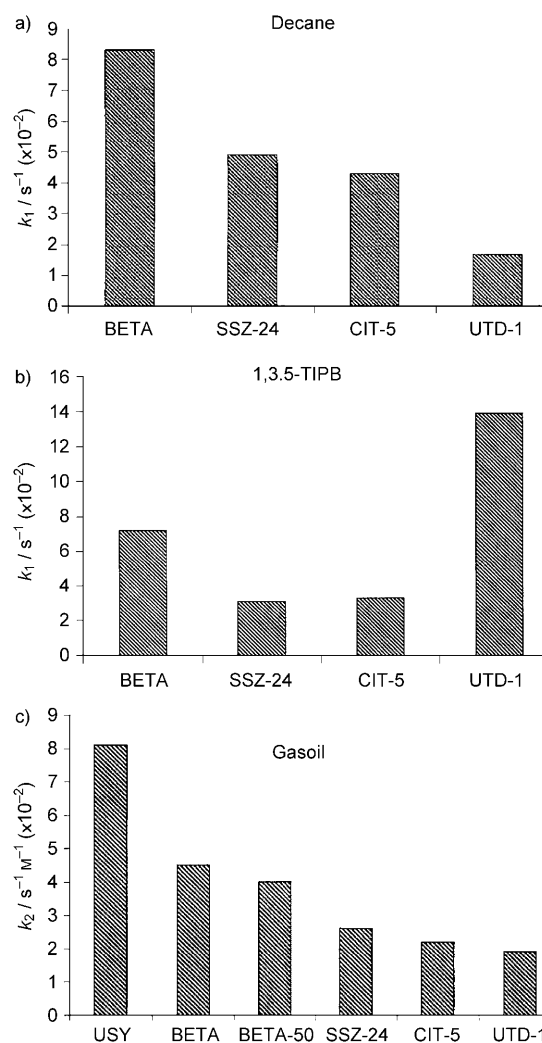


Figure 17. a) First-order kinetic rate constants (k_1) for *n*-decane cracking over Beta, SSZ-24, CIT-5, and UTD-1. b) First-order kinetic rate constants for 1,3,5-triisopropylbenzene cracking over Beta, SSZ-24, CIT-5, and UTD-1. c) Second-order kinetic rate constants (k_2) for gas oil cracking over SSZ-24, CIT-5, and UTD-1 and other zeolites. Taken from Ref. [186].

of UTD-1 compared with SSZ-24 and CIT-5. The catalytic activity of UTD-1 is even higher than for zeolite Beta which forms smaller crystallites than UTD-1, thus an important contribution to the observed catalytic activity of zeolite Beta comes from the external surface area.

The results given in Figure 17c clearly show that the gas oil cracking activity is much higher for the 3D USY and Beta zeolites than for any of the other three 1D zeolites. This situation could be the result of the 3D system of pores in the USY and Beta zeolites that will not be blocked by coke as easily as the 1D pore zeolites. Apparently, the extra-large-pore size of UTD-1 is limited to convert only the largest molecules present in the vacuum gas oil feed and, furthermore, does not improve its resistance to coke formation. Thus, 1D extra-large-pore zeolites are of limited interest for fluid catalytic cracking, but could be of interest for processes where coke formation is lower, such as dehydrocyclization, hydro-

isomerization, and hydrocracking of *n*-paraffin, or even naphthalene alkylation.

It is becoming apparent that 1D extra-large-pore zeolites have advantages in selective transformations in the fields of petrochemical and chemicals. Indeed, Sugi et al.^[187] have investigated the alkylation of biphenyl with 1D 12R (Mordenite, ZSM-12, SSZ-24, SAPO-5, SSZ-31, SSZ-42) and 1D 14R (UTD-1, CIT-5, SSZ-53) zeolites as shape selective catalysts. Herein, we will concentrate on their work with 14R pore zeolites.^[187e] In their work, several acid forms of CIT-5, UTD-1, and SSZ-53 were used as catalysts, and their behaviors were compared with that of the 1D 12R Mordenite. Three reactions, including isopropylation, *sec*-butylation, and *tert*-butylation of biphenyl (BP) were examined over these zeolites between 150–350 °C. As seen in Figure 18, the highest

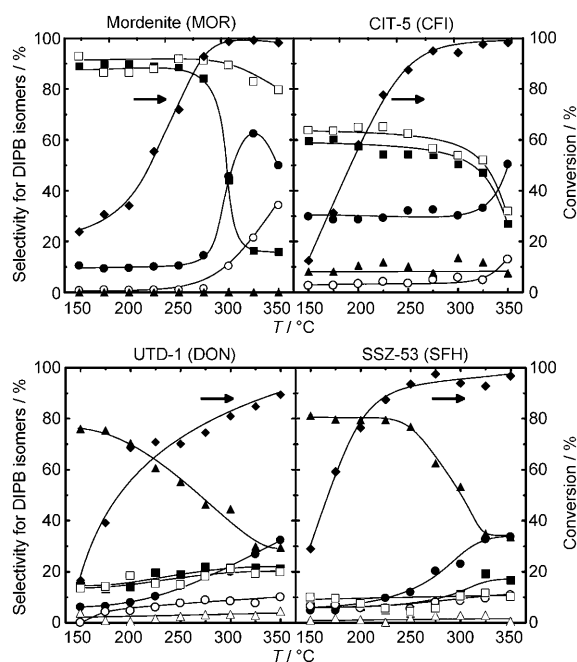


Figure 18. The influence of reaction temperature on the isopropylation of biphenyl over Mordenite CIT-5, UTD-1, and SSZ-53. Bulk product ■ 4,4'-DIPB; ● 3,4'-DIPB; ○ 3,3'-DIPB; ▲ 2,x'-DIPB; ◆ conversion. Encapsulated products □ 4,4'-DIPB, △ = 2,x'-DIPB; DIBP = diisopropylbiphenyl. Taken from Ref. [187e].

selectivity for the least-bulky of the diisopropylbiphenyl (DIPB) isomers was 85–90% over Mordenite (below 250 °C), and 50–60% for CIT-5 (up to 300 °C). These results show that shape selective catalysis occurs inside Mordenite and CIT-5 channels and that bulky DIPB isomers are excluded from the channels by steric restrictions. The decrease in selectivity to 4,4'-DIPB in Mordenite and CIT-5 after a certain temperature value, is due to the isomerization of 4,4'-DIPB on the external acid site. If only the encapsulated products are considered then the selectivity of 4,4'-DIPB in Mordenite remains high, even for temperatures as high as 350 °C. The selectivity for the linear DIPB isomer was less than 20% in the isopropylation of biphenyl over UTD-1 and SSZ-53. Over these zeolites the predominant products were the bulky and thermodynamically

unstable 2,2'-DIPB, 2,3'-DIPB, and 2,4'-DIPB (2,x'-DIPB) which are the kinetically controlled products at the lower temperature, while the yields of the thermodynamically more stable 3,4'-DIPB, 3,3'-DIPB, and 4,4'-DIPB isomers, increase when increasing the reaction temperature. The low yield of the linear isomer with both zeolites implies that the channels of UTD-1 and SSZ-53 are too large to select the less-bulky linear product. The reaction with bulkier alkylation agents, for example, 1-butene and 2-methylpropene were also studied and a similar tendency was found. Nevertheless, and as can be seen in Figure 19, the selectivity for all four zeolites increases when bulkier alkylation agents are employed.

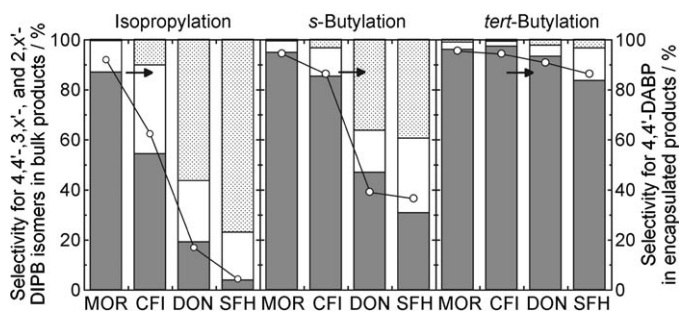


Figure 19. The selectivity for DABP (dialkylbiphenyl) isomers in the alkylation of biphenyl over zeolites. Reaction condition: temperature: 250 °C. gray bar 4,4'-DABP; white bar 3,x'-DABP (3,4,0-, 3,3,0-, and 3,5-); dotted bar 2,x'-DABP (2,2,0-, 2,3,0-, and 2,4,0-); ○ 4,4'-DABP (encapsulated products). Taken from Ref. [187e].

CIT-5, UTD-1, and SSZ-53 have 14R pore entrances with different channel structures: CFI(CIT-5) has slightly corrugated 1D channels with 16R cavities (pore entrance: 0.72×0.75 nm),^[45,69] DON(UTD-1) has straight 1D channels (pore entrance: 0.74×0.95 nm),^[44,69] and SFH(SSZ-53) has largely corrugated 1D channels with 22R cavities (pore entrance: 0.66×0.88 nm).^[47,69] The differences between the 14R zeolites indicate that the reaction space inside the channels increases in the order CFI \ll DON \ll SFH, and the size of pore entrance increases in the order: CFI < SFH < DON. These differences suggest that the steric restriction within the channels decreases in the order CFI \gg DON > SFH. These factors should account for the differences in the exclusion of the bulky DABP isomer from the channels during the alkylation.

Beside Brønsted acid sites, a Lewis acid Ti^{4+} site, able to catalyze oxidation reactions using peroxides, was introduced in UTD-1. For instance, Balkus et al. reported that Ti-UTD-1 can be an effective catalyst for the oxidation of alkanes, alkenes, and phenols using either hydrogen peroxide or the bulkier *tert*-butylhydroperoxide as the oxidant. The 14R channel structure also allows the conversion of larger substrates, such as 2,6-di-*tert*-butylphenol.^[188]

When considering zeolites with large pore diameters and the possibility to support catalytically active sites, the catalytic results obtained with ECR-34 merits special mention.^[48] A bifunctional metal–acid catalyst was prepared, showing interesting hydroisomerization–hydrocracking properties for *n*-alkanes owing to its pore dimensions and mild acidity.

The synthesis of a 3D extra-large-pore zeolite, such as ITQ-15 (IM-12) and ITQ-33, can open new possibilities for catalysis, especially in the domain of oil refining and fine chemicals. Thus, the catalytic cracking process (FCC), currently based on zeolite Y, converts bulky hydrocarbons into more valuable fractions, such as light olefins and liquid fuels. It would be of interest for the field to find new zeolites with larger pores and stable structures. Preliminary results^[52] have shown that ITQ-33 has an activity for conversion of a vacuum gas oil that is comparable to that of a USY zeolite. Another remarkable fact is that ITQ-33 is simultaneously highly selective to diesel (LCO) and propylene (Table 9), a feature

Table 9: Catalytic cracking of Arabian light vacuum gas oil at 500 °C and 60 s time on-stream. Taken from Ref. [52].

Catalyst	Conversion [%]	Yields [%]			Molar ratio	
		diesel	gasoline	propylene	Propylene/ propane	Isobutene/ isobutane
USY ^[a]						
Catalyst/oil = 0.62	92.5	15.7	40.4	4.7	1	0.1
Catalyst/oil = 0.47	88.3	19.5	39.5	4.4	1.3	0.1
ITQ-33						
Catalyst/oil = 0.70	89.2	22.6	34.5	4.2	1.9	0.4
Beta						
Catalyst/oil = 0.70	84	14.1	32.3	7.5	1.9	0.5
USY + 20%ZSM-5	87	17	33.2	7.2	1.5	0.3
ITQ-33 + 20% ZSM-5	86.1	23.3	25.1	9	3.7	1.1

[a] For the USY catalyst, unit cell size is 2.432 nm. The higher catalyst-to-oil ratio used with USY is close to that used for ITQ-33 and Beta, and gives a comparison of catalyst activity. The lower ratio allows us to achieve a level of conversion similar to other catalysts; this ratio is much better for comparing selectivities. The conversion is to diesel + gasoline + gases + coke. For diesel the boiling point is 216.1–359.0 °C and for gasoline it is 36.0–216.1 °C.

which is related to the combination of 18R and 10R channels in the same structure.

Since ITQ-33 is a germano-aluminium-silicate, its acidic properties could be unusual and worth studying. To do that, a self-supporting wafer of Al-ITQ-33 ($T^{VI}/T^{III} = 20$) was calcined in the IR cell at 673 K and 10^{-2} Pa. When all the OSDA molecules were removed, the IR spectrum in the OH stretching region showed the presence of three bands at 3740, 3675, and 3608 cm^{-1} (Figure 20a, upper spectrum) associated with the presence of silanols, germanols, and bridging hydroxy groups, respectively. After pyridine molecules were adsorbed at room temperature and then desorbed at 423 K in vacuum to remove the physically adsorbed ones (see Figure 20a, lower spectrum), some changes in the IR spectrum were visible. The intensity of the bands associated with silanol and germanol groups (3740 and 3675 cm^{-1}) increased, indicating that the introduction of pyridine and subsequent desorption causes some hydrolysis of Si-O-Ge bonds. The adsorption of pyridine also causes the disappearance of the band associated with bridging OH groups, as a result of the protonation of the base. Indeed, the IR spectrum of the pyridine remaining adsorbed after evacuation at 423 K clearly showed the presence of bands at 1545 and 1638 cm^{-1} , which are associated with protonated pyridine (see Figure 20b, lower spectrum). The same spectrum also shows IR bands at 1452, 1610, and 1622 cm^{-1} that can be associated with

pyridine coordinated to Lewis acid sites. More specifically, the band at 1622 cm^{-1} should correspond to pyridine coordinated to extra-framework aluminium as a Lewis acid, and the band at 1610 cm^{-1} , which is detected exclusively in germanium-containing zeolites, indicates sites of weaker Lewis acidity and should be associated with pyridine coordinated to Ge. Notice that after evacuation at 523 K (Figure 20b, middle), all the pyridine molecules bound to Brønsted (bridging hydroxy groups) and Lewis acids remained, except for those pyridine molecules that were associated with the weaker Lewis acidic Ge centers. The relative intensity of the 1545 cm^{-1} pyridine band after desorption at 423 and 523 K (Figure 20b) clearly shows that an important fraction of the Brønsted acid sites cannot retain the pyridine adsorbed at the higher temperatures, indicating that ITQ-33 presents medium to strong Brønsted acidity. Indeed, at a desorption temperature of 623 K, only a very small amount of pyridine remained protonated on strong acid sites. When the catalytic behavior of ITQ-33 is compared with that of UTD-1 and Beta zeolites for dealkylating diisopropylbenzene (DIPB), the results (Figure 21) indicate that the intrinsic activity, that is, the activity per Al^{III} , is higher for the aluminosilicate Beta ($\text{Si}/\text{Al}=30$) and UTD-1 ($\text{Si}/\text{Al}=80$) than for ITQ-33 ($T^{IV}/T^{III}=20$). This is

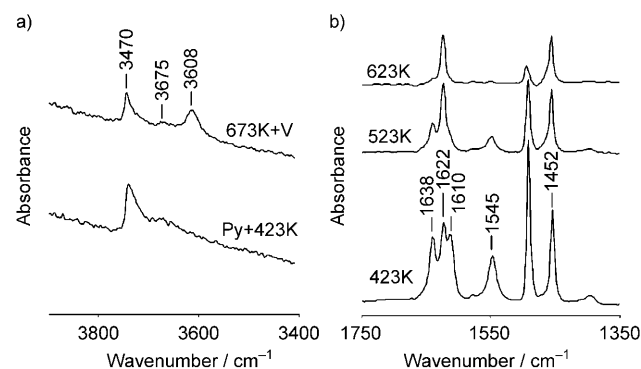


Figure 20. Acid properties of Al-ITQ-33 zeolite determined by IR spectroscopy of pyridine adsorption/stepwise desorption at different temperatures. a) Stretching hydroxy region of the IR spectra upon thermal treatment at 673 K under vacuum (upper spectrum) and after adsorbing pyridine and subsequent desorption by heating at 423 K (lower spectrum). b) C–C stretching region of the adsorbed pyridine upon desorption at 423 K (lower), 523 K (middle), and 623 K (upper). The spectra are offset for clarity. Taken from Ref. [145].

because of the higher electronegativity of the UTD-1 and Beta zeolites. However in the case of the bulkier 1,3,5-triisopropylbenzene (TIPB), UTD-1 with 14R pores gave a higher activity than Beta despite having the much higher Si/Al ratio ($\text{Si}/\text{Al} = 80$). Finally, ITQ-33 with 18R pores gave the highest activity for the cracking of the bulkiest molecule.

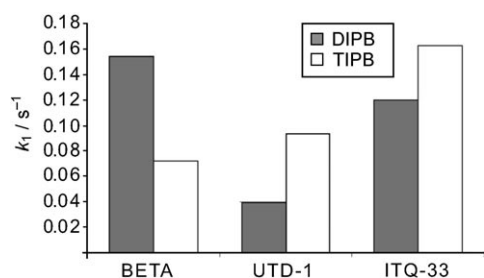


Figure 21. First-order kinetic rate constants for 1,3-diisopropylbenzene (DIPB) and 1,3,5-triisopropylbenzene (TIPB) cracking over zeolite Beta, UTD-1, and ITQ-33. Taken from Ref. [145].

It appears then that ITQ-33 can be an excellent catalyst for processes requiring mild acidities and extra-large pores. The benefit of these two properties is shown by the results obtained for benzene alkylation with propylene. Figure 22 shows that ITQ-33 is not only very active, but it is also more

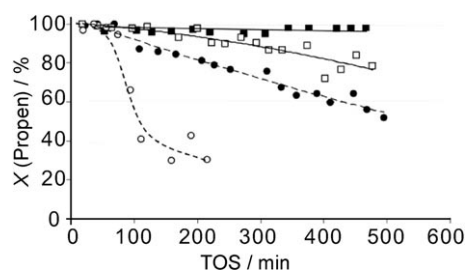


Figure 22. Propylene conversion for zeolite ITQ-33 (squares) and Beta (circles) at 398 K, 3.5 MPa, mol ratio benzene/propylene = 3.5 and weight hourly space velocity (WHSV) of 12 (black symbols) and 24 h⁻¹ (open symbols). TOS = time on stream. Taken from Ref. [145].

resistant to deactivation than zeolite Beta. Although commercial processes deal with this problem by combining reaction/regeneration cycles, there is a need to minimize olefin oligomerization and coking so as to increase catalyst life. The special microporous structure of ITQ-33 favors the formation and diffusion of the alkylation products while reducing the undesired propylene oligomerization.

Besides its high activity, ITQ-33 is highly selective for alkylation products. Nevertheless, the large 18R pores allow the formation of polyalkylated products, such as diisopropylbenzene and triisopropylbenzene, in larger proportions than with zeolite Beta (Table 10).

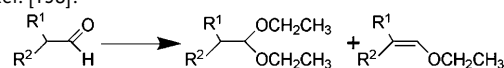
Table 10: Conversion X and product selectivity S [wt%] for the alkylation of benzene with propylene using zeolites ITQ-33 and Beta. Taken from Ref. [145].^[a]

Cat.	X	$S(\text{cumene})$	$S(\text{DIPB})$	$S(\text{TIPB})$
	WHSV ^[b] = 12 h ⁻¹			
ITQ-33	98.6	76.5	17.3	3.7
Beta	95.7	90	6.9	< 0.1
	WHSV ^[b] = 24 h ⁻¹			
ITQ-33	98.7	63.8	23	7.8
Beta	78.2	86.9	9	0.7

[a] $T = 398$ K, $P = 3.5$ MPa, mol ratio benzene/propylene = 3.5, time on stream 1 h. [b] WHSV = weight hourly space velocity.

Al-ITQ-37 zeolite with the largest pore reported to date has Brønsted acidity upon pyridine adsorption. Acetalization reactions require catalysts with mild acidity, and the acetals formed can be of interest for fine chemical industries.^[189] Thus, we have performed acetalization of aldehydes of different molecular sizes with triethyl orthoformate using ITQ-37 as a catalyst to show the benefits of the extra large pores. The activity of ITQ-37 was compared with that of zeolite Beta (Si/Al = 50) with a similar crystallite size. For the smaller aldehyde (heptanal) that could diffuse in the pores of Beta, both materials gave a similar initial activity. However for a larger aldehyde (diphenylacetaldehyde), the initial activity of ITQ-37 was almost three times that of Beta (Table 11). This result indicates the presence of larger exploitable pores in ITQ-37 than in zeolite Beta. Furthermore, the selectivity for acetal at high conversion is much better for ITQ-37 when using the bulkier aldehyde.

Table 11: Catalytic re-acetalization of aldehydes of different molecular sizes with triethyl orthoformate, using zeolites Beta and ITQ-37. Taken from Ref. [158].^[a]



Zeolite	Heptanal TOF ^[b]	Diphenylacetaldehyde	
		TOF ^[b]	S_A ^[c] (6 h)
Beta (Si/Al = 50)	276	18	30
ITQ-37 ((Si,Ge)/Al = 70)	270	53	49

[a] Heptanal: $\text{R}^1 = \text{CH}_3(\text{CH}_2)_4$, $\text{R}^2 = \text{H}$; Diphenylacetaldehyde: $\text{R}^1 = \text{R}^2 = \text{Ph}$. [b] mol converted/(mol Al h). [c] S_A = selectivity for acetal.

10. Summary and Outlook

It appears that there is not a thermodynamic limitation to the synthesis of extra-large-pore zeolites. Advances in the understanding of the role of the different synthesis variables: OSDA, gel concentration, mineralizer, and framework isomorphous substitutions has allowed silica-based zeolites with extra-large pores to be synthesized. However, for synthesizing zeolites with the largest pores to date, the presence of cations such as Ga, Be, and Ge, has been required. This situation shows the important structure-directing effect played by framework cations, and new structures will be achieved working along this direction. For practical purposes, the challenge remains in synthesizing 3D extra-large-pore zeolites and mesoporous zeolites, such as ITQ-37, in the form of aluminosilicates or borosilicates. For doing this it is possible to use the zeolite database for hypothetical structures, select the theoretically most feasible structures, and then design templates by maximizing the Van der Waals interactions between the template and the framework. This, which is logical and is easily said, it is not easy to do

lites and mesoporous zeolites, such as ITQ-37, in the form of aluminosilicates or borosilicates. For doing this it is possible to use the zeolite database for hypothetical structures, select the theoretically most feasible structures, and then design templates by maximizing the Van der Waals interactions between the template and the framework. This, which is logical and is easily said, it is not easy to do

in practice. However, we believe more research should be done in these directions.

To date, the potential catalytic applications of 1D and with 3D extra-large-pore zeolites, such as ITQ-33 and ITQ-37 have already been demonstrated. We hope that many researchers who have gained experience working with structured mesoporous materials will apply their accumulated knowledge in field of zeolites and zeolitic materials. More creativity and the help of high-throughput synthesis techniques should allow many new and potentially useful zeolites to be harvested.

We acknowledge financial support from Spanish Government (Mat-2006-14274-C02-01); Prometeo Project from the Generalitat Valenciana, and Fundaci3n Areces. J.X.J. thanks the China Scholarship Council and ITQ for scholarships. J.H.Y. thanks the support from the the State Basic Research Project of China (Grants: 2006CB806103 and 2007CB936402), and the Major International Joint Research Project of China. This work has been developed in the framework of the agreement between the ITQ (UPV-CSIC) and the College of Chemistry from Jilin University.

Received: July 21, 2009

- [1] P. B. Venuto, *Microporous Mater.* **1994**, *2*, 297.
- [2] A. Corma, *J. Catal.* **2003**, *216*, 298–312.
- [3] A. Corma, *Chem. Rev.* **1995**, *95*, 559–614.
- [4] M. E. Davis, *Nature* **2002**, *417*, 813–821.
- [5] M. E. Davis, *Chem. Eur. J.* **1997**, *3*, 1745–1750.
- [6] M. E. Davis, *Chem. Ind.* **1992**, 137–139.
- [7] J. L. Casci, *Stud. Surf. Sci. Catal.* **1994**, *85*, 329–356.
- [8] M. E. Davis, P. E. Hathaway, C. Montes, *Zeolites* **1989**, *9*, 436.
- [9] P. B. Moore, J. Shen, *Nature* **1983**, *306*, 356.
- [10] M. E. Davis, C. Saldarriaga, C. Montes, J. Garces, C. Crowder, *Nature* **1988**, *331*, 698.
- [11] E. T. C. Vogt, J. W. Richardson, *J. Solid State Chem.* **1990**, *87*, 469.
- [12] Q. S. Huo, R. R. Xu, S. G. Li, Z. G. Ma, J. M. Thomas, R. H. Jones, A. M. Chippindale, *J. Chem. Soc. Chem. Commun.* **1992**, 875–876.
- [13] M. Estermann, L. B. McCusker, C. Baerlocher, A. Merrouche, H. Kessler, *Nature* **1991**, *352*, 320–323.
- [14] T. Loiseau, G. Férey, *J. Solid State Chem.* **1994**, *111*, 403–415.
- [15] T. Loiseau, G. Férey, *J. Mater. Chem.* **1996**, *6*, 1073–1074.
- [16] C. Sassoie, J. Marrot, T. Loiseau, G. Férey, *Chem. Mater.* **2002**, *14*, 1340–1347.
- [17] C. Sassoie, T. Loiseau, F. Taulelle, G. Férey, *Chem. Commun.* **2000**, 943–944.
- [18] L. Beitone, J. Marrot, T. Loiseau, G. Férey, M. Henry, C. Huguenard, A. Gansmuller, F. Taulelle, *J. Am. Chem. Soc.* **2003**, *125*, 1912–1922.
- [19] S. J. Weigel, R. E. Morris, G. D. Stucky, A. K. Cheetham, *J. Mater. Chem.* **1998**, *8*, 1607–1611.
- [20] R. I. Walton, F. Millange, T. Loiseau, D. O'Hare, G. Férey, *Angew. Chem.* **2000**, *112*, 4726–4729; *Angew. Chem. Int. Ed.* **2000**, *39*, 4552–4555.
- [21] A. M. Chippindale, K. J. Peacock, A. R. Cowley, *J. Solid State Chem.* **1999**, *145*, 379–386.
- [22] C. H. Lin, S. L. Wang, K. H. Lii, *J. Am. Chem. Soc.* **2001**, *123*, 4649–4650.
- [23] M. I. Khan, L. M. Meyer, R. C. Haushalter, A. L. Schweitzer, J. Zubietta, J. L. Dye, *Chem. Mater.* **1996**, *8*, 43–53.
- [24] N. Guillou, Q. Gao, M. Nogues, R. E. Morris, M. Hervieu, G. Férey, A. K. Cheetham, *C. R. Acad. Sci. Paris Ser.* **1999**, *2*, 387–392.
- [25] N. Guillou, Q. Gao, P. M. Forster, J. S. Chang, M. Nogués, S. E. Park, G. Férey, A. K. Cheetham, *Angew. Chem.* **2001**, *113*, 2913; *Angew. Chem. Int. Ed.* **2001**, *40*, 2831.
- [26] W. T. A. Harrison, *J. Solid State Chem.* **2001**, *160*, 4–7.
- [27] W. T. A. Harrison, M. L. F. Phillips, T. M. Nenoff, *Int. J. Inorg. Mater.* **2001**, *3*, 1033–1038.
- [28] Z. E. Lin, J. Zhang, S. T. Zheng, G. Y. Yang, *J. Mater. Chem.* **2004**, *14*, 1652–1655.
- [29] W. B. Chen, N. Li, S. H. Xiang, *J. Solid State Chem.* **2004**, *177*, 3229–3234.
- [30] R. K. Chiang, N. T. Chuang, *J. Solid State Chem.* **2005**, *178*, 3040–3045.
- [31] L. Zhao, J. Y. Li, P. Chen, G. H. Li, J. H. Yu, R. R. Xu, *Chem. Mater.* **2008**, *20*, 17–19.
- [32] a) J. Liang, J. Y. Li, J. H. Yu, P. Chen, Q. R. Fang, F. X. Sun, R. R. Xu, *Angew. Chem.* **2006**, *118*, 2608–2610; *Angew. Chem. Int. Ed.* **2006**, *45*, 2546–2548; b) J. Y. Li, L. Li, J. Liang, P. Chen, J. H. Yu, Y. Xu, R. R. Xu, *Cryst. Growth Des.* **2008**, *8*, 2318–2323.
- [33] Y. L. Lai, K. H. Lii, S. L. Wang, *J. Am. Chem. Soc.* **2007**, *129*, 5350–5351.
- [34] J. Zhu, X. H. Bu, P. Y. Feng, G. D. Stucky, *J. Am. Chem. Soc.* **2000**, *122*, 11563–11564.
- [35] J. Plévert, T. M. Gentz, A. Laine, H. L. Li, V. G. Young, O. M. Yaghi, M. O'Keeffe, *J. Am. Chem. Soc.* **2001**, *123*, 12706–12707.
- [36] Y. M. Zhou, H. G. Zhu, Z. X. Chen, M. Q. Chen, Y. Xu, H. Y. Zhang, D. Y. Zhao, *Angew. Chem.* **2001**, *113*, 2224; *Angew. Chem. Int. Ed.* **2001**, *40*, 2166.
- [37] M. E. Medina, E. G. Puebla, M. A. Monge, N. Snejkko, *Chem. Commun.* **2004**, 2868–2869.
- [38] Z. E. Lin, J. Zhang, J. T. Zhao, S. T. Zheng, C. Y. Pan, G. M. Wang, G. Y. Yang, *Angew. Chem.* **2005**, *117*, 7041; *Angew. Chem. Int. Ed.* **2005**, *44*, 6881.
- [39] X. D. Zou, T. Conradsson, M. Klingstedt, M. S. Dadachov, M. O'Keeffe, *Nature* **2005**, *437*, 716–719.
- [40] K. E. Christensen, C. Bonneau, M. Gustafsson, L. Shi, J. L. Sun, J. Grins, K. Jansson, I. Sibile, B. L. Su, X. D. Zou, *J. Am. Chem. Soc.* **2008**, *130*, 3758–3759.
- [41] K. E. Christensen, L. Shi, T. Conradsson, T. Z. Ren, M. S. Dadachov, X. D. Zou, *J. Am. Chem. Soc.* **2006**, *128*, 14238–14239.
- [42] X. Y. Ren, Y. Li, Q. H. Pan, J. H. Yu, R. R. Xu, Y. Xu, *J. Am. Chem. Soc.* **2009**, *131*, 14128–14129.
- [43] M. O'Keeffe, O. M. Yaghi, *Chem. Eur. J.* **1999**, *5*, 2796–2801.
- [44] a) C. C. Freyhardt, M. Tsapatsis, R. F. Lobo, K. J. Balkus, Jr., M. E. Davis, *Nature* **1996**, *381*, 295; b) R. F. Lobo, M. Tsapatsis, C. C. Freyhardt, S. Khodabandeh, P. Wagner, C. Y. Chen, K. J. Balkus, S. I. Zones, M. E. Davis, *J. Am. Chem. Soc.* **1997**, *119*, 8474–8484; c) T. Wessels, C. Baerlocher, L. B. McCusker, E. J. Creighton, *J. Am. Chem. Soc.* **1999**, *121*, 6242–6247.
- [45] P. Wagner, M. Yoshikawa, M. Lovallo, K. Tsuji, M. Taspatsis, M. E. Davis, *Chem. Commun.* **1997**, 2179–2180.
- [46] A. K. Cheetham, H. Fjellvåg, T. E. Gier, K. O. Kongshaug, K. P. Lillerud, G. D. Stucky, *Stud. Surf. Sci. Catal.* **2001**, *135*, 158.
- [47] A. Burton, S. Elomari, C. Y. Chen, R. C. Medrud, I. Y. Chan, L. M. Bull, C. Kibby, T. V. Harris, S. I. Zones, E. S. Vittoratos, *Chem. Eur. J.* **2003**, *9*, 5737–5748.
- [48] K. G. Strohmaier, D. E. W. Vaughan, *J. Am. Chem. Soc.* **2003**, *125*, 16035–16039.
- [49] a) A. Corma, M. J. Díaz-Cabañas, F. Rey, Sp. Pat. ES2186487, **2000**; b) A. Corma, M. J. Díaz-Cabañas, F. Rey, PCT Int. Appl. WO0203820, **2002**.

- [50] A. Corma, M. J. Díaz-Cabañas, F. Rey, S. Nicolopoulos, K. Boulahya, *Chem. Commun.* **2004**, 1356–1357.
- [51] J. L. Paillaud, B. Harbuzaru, J. Patarin, N. Bats, *Science* **2004**, *304*, 990–992.
- [52] A. Corma, M. J. Díaz-Cabañas, J. L. Jordá, C. Martínez, M. Moliner, *Nature* **2006**, *443*, 842–845.
- [53] D. W. Breck, *Zeolite Molecular Sieves: Structure, Chemistry, and Use*, Wiley, New York, **1974**.
- [54] R. M. Barrer, H. Villiger, *Z. Kristallogr.* **1969**, *128*, 352.
- [55] J. V. Smith, W. J. Dytrych, *Nature* **1984**, *309*, 607.
- [56] J. V. Smith, *Chem. Rev.* **1988**, *88*, 149.
- [57] a) M. W. Deem, J. M. Newsam, *Nature* **1989**, *342*, 260; b) M. W. Deem, J. M. Newsam, *J. Am. Chem. Soc.* **1992**, *114*, 7189; c) M. Falcioni, M. W. Deem, *J. Chem. Phys.* **1999**, *110*, 1754; d) D. J. Earl, M. W. Deem, *Ind. Eng. Chem. Res.* **2006**, *45*, 5449.
- [58] a) M. M. J. Treacy, K. H. Randall, S. Rao, J. A. Perry, D. J. Chadi, *Z. Kristallogr.* **1997**, *212*, 768; b) M. M. J. Treacy, I. Rivin, E. Balkovsky, K. H. Randall, M. D. Foster, *Microporous Mesoporous Mater.* **2004**, *74*, 121.
- [59] a) O. D. Friedrichs, A. W. M. Dress, D. H. Huson, J. Klinowski, A. L. Mackay, *Nature* **1999**, *400*, 644; b) M. D. Foster, A. Simperler, R. G. Bell, O. D. Friedrichs, F. A. A. Paz, J. Klinowski, *Nat. Mater.* **2004**, *3*, 234; c) M. D. Foster, O. D. Friedrichs, R. G. Bell, F. A. A. Paz, J. Klinowski, *J. Am. Chem. Soc.* **2004**, *126*, 9769; d) A. Simperler, M. D. Foster, O. D. Friedrichs, R. G. Bell, F. A. A. Paz, J. Klinowski, *Acta Crystallogr. Sect. B* **2005**, *61*, 263.
- [60] a) C. Mellot-Draznieks, J. M. Newsam, A. M. Gorman, C. M. Freeman, G. Férey, *Angew. Chem.* **2000**, *112*, 2358; *Angew. Chem. Int. Ed.* **2000**, *39*, 2270; b) C. Mellot-Draznieks, S. Girard, G. Férey, J. C. Schön, Z. Cancarevic, M. Jansen, *Chem. Eur. J.* **2002**, *8*, 4102; c) C. Mellot-Draznieks, S. Girard, G. Férey, *J. Am. Chem. Soc.* **2002**, *124*, 15326.
- [61] a) Y. Li, J. H. Yu, D. H. Liu, W. F. Yan, R. R. Xu, Y. Xu, *Chem. Mater.* **2003**, *15*, 2780–2785; b) Y. Li, J. H. Yu, Z. P. Wang, J. N. Zhang, M. Guo, R. R. Xu, *Chem. Mater.* **2005**, *17*, 4399–4405; c) Y. Li, J. H. Yu, J. X. Jiang, Z. P. Wang, J. N. Zhang, R. R. Xu, *Chem. Mater.* **2005**, *17*, 6086–6093.
- [62] S. M. Woodley, C. R. A. Catlow, P. D. Battle, J. D. Gale, *Chem. Commun.* **2004**, 22.
- [63] M. D. Foster, M. M. J. Treacy, <http://www.hypotheticalZeolites-net/>.
- [64] C. Baerlocher, F. Gramm, L. Massüger, L. B. McCusker, Z. B. He, S. Hovmöller, X. D. Zou, *Science* **2007**, *315*, 1113–1116.
- [65] F. Gramm, C. Baerlocher, L. B. McCusker, S. J. Warrender, P. A. Wright, B. Han, S. B. Hong, Z. Liu, T. Ohsuna, O. Terasaki, *Nature* **2006**, *444*, 79–81.
- [66] Y. Li, J. H. Yu, R. R. Xu, C. Baerlocher, L. B. McCusker, *Angew. Chem.* **2008**, *120*, 4473–4477; *Angew. Chem. Int. Ed.* **2008**, *47*, 4401–4405.
- [67] Y. Li, J. H. Yu, R. R. Xu, <http://mezeopor.jlu.edu.cn/>.
- [68] N. F. Zheng, X. H. Bu, B. Wang, P. Y. Feng, *Science* **2002**, *298*, 2366–2369.
- [69] a) C. Baerlocher, L. B. McCusker, D. H. Olson, *Atlas of Zeolite Framework Types*, 5th ed., Elsevier, Amsterdam, **2001**; b) C. Baerlocher, L. B. McCusker, D. H. Olson, *Atlas of Zeolite Framework Types*, 6th ed., Elsevier, Amsterdam, **2007**; c) <http://izasc.ethz.ch/fmi/xsl/IZA-SC/ft.xml>.
- [70] G. O. Brunner, W. M. Meier, *Nature* **1989**, *337*, 146.
- [71] M. A. Zwijnenburg, R. G. Bell, *Chem. Mater.* **2008**, *20*, 3008–3014.
- [72] M. M. Helmkamp, M. E. Davis, *Annu. Rev. Mater. Sci.* **1995**, *25*, 161–192.
- [73] P. M. Piccione, S. Yang, A. Navrotsky, M. E. Davis, *J. Phys. Chem. B* **2002**, *106*, 3629–3638.
- [74] I. Petrovic, A. Navrotsky, M. E. Davis, S. I. Zones, *Chem. Mater.* **1993**, *5*, 1805–1813.
- [75] P. M. Piccione, C. Laberty, S. Yang, M. A. Cambor, A. Navrotsky, M. E. Davis, *J. Phys. Chem. B* **2000**, *104*, 10001–10011.
- [76] A. Navrotsky, I. Petrovic, Y. Hu, C. Y. Chen, M. E. Davis, *Microporous Mater.* **1995**, *4*, 95–98.
- [77] G. V. Gibbs, personal communication, **1998**.
- [78] Q. Li, A. Navrotsky, F. Rey, A. Corma, *Microporous Mesoporous Mater.* **2003**, *64*, 127–133.
- [79] a) M. A. Zwijnenburg, S. T. Bromley, J. C. Jansen, T. Maschmeyer, *Chem. Mater.* **2004**, *16*, 12; b) M. A. Zwijnenburg, S. T. Bromley, M. D. Foster, R. G. Bell, O. D. Friedrichs, J. C. Jansen, T. Maschmeyer, *Chem. Mater.* **2004**, *16*, 3809.
- [80] G. Sastre, A. Corma, *J. Phys. Chem. B* **2006**, *110*, 17949–17959.
- [81] S. L. Lawton, W. J. Rohrbach, *Science* **1990**, *247*, 1319.
- [82] R. M. Barrer, P. J. Denny, *J. Chem. Soc.* **1961**, 983.
- [83] R. Aiello, R. M. Barrer, *J. Chem. Soc. A* **1970**, 1470.
- [84] G. T. Kerr, *Inorg. Chem.* **1966**, *5*, 1537.
- [85] H. Gies, *Inclusion Compounds, Vol. 5*, Academic Press, London, **1995**.
- [86] H. Gies, B. Marler, *Zeolites* **1992**, *12*, 42.
- [87] R. F. Lobo, S. I. Zones, M. E. Davis, *J. Inclusion Phenom. Mol. Recognit. Chem.* **1995**, *21*, 47–78.
- [88] S. I. Zones, Y. Nakagawa, J. W. Rosenthal, *Zeolites* **1994**, *11*, 81.
- [89] F. Delprato, L. Delmotte, J. L. Guth, L. Huve, *Zeolites* **1990**, *10*, 546.
- [90] a) A. B. Schwartz, Ger. Offen. DE 2117117, **1971**; b) D. L. Dorset, K. G. Strohmaier, C. E. Kliewer, A. Corma, M. J. Díaz-Cabañas, F. Rey, C. J. Gilmore, *Chem. Mater.* **2008**, *20*, 5325–5331.
- [91] D. L. Dorset, G. J. Kennedy, K. G. Strohmaier, M. J. Diaz-Cabanias, F. Rey, A. Corma, *J. Am. Chem. Soc.* **2006**, *128*, 8862–8867.
- [92] M. A. Cambor, C. Corell, A. Corma, M. J. Díaz-Cabañas, S. Nicolopoulos, J. M. G. Calbet, M. V. Regí, *Chem. Mater.* **1996**, *8*, 2415.
- [93] M. A. Cambor, A. Corma, M. J. Díaz-Cabañas, *J. Phys. Chem. B* **1998**, *102*, 44–51.
- [94] A. Cantín, A. Corma, M. J. Diaz-Cabañas, J. L. Jordá, M. Moliner, *J. Am. Chem. Soc.* **2006**, *128*, 4216–4217.
- [95] A. Corma, F. Rey, J. Rius, M. J. Sabater, S. Valencia, *Nature* **2004**, *431*, 287–290.
- [96] A. W. Burton, S. I. Zones, S. Elomari, *Curr. Opin. Colloid Interface Sci.* **2005**, *10*, 211–219.
- [97] A. W. Burton, S. I. Zones, *Microporous Mesoporous Mater.* **2006**, *90*, 129–144.
- [98] M. E. Davis, R. F. Lobo, *Chem. Mater.* **1992**, *4*, 756–768.
- [99] R. A. Van Nordstand, D. S. Santilli, S. I. Zones, *ACS Symp. Ser.* **1988**, *368*, 236.
- [100] a) J. P. Arhancet, M. E. Davis, *Chem. Mater.* **1991**, *3*, 567; b) M. N. Anderson, K. S. Pachis, F. Prebin, S. W. Carr, O. Terasaki, T. Ohsuna, V. Alfredson, *J. Chem. Soc. Chem. Commun.* **1991**, 1660; c) F. Delprato, J. L. Delmotte, J. L. Guth, L. Huve, *Zeolites* **1990**, *10*, 546; d) M. J. Annen, D. Young, J. P. Arhancet, M. E. Davis, S. Schramm, *Zeolites* **1991**, *11*, 98.
- [101] P. Wagner, Y. Nakagawa, G. S. Lee, M. E. Davis, S. Elomari, R. C. Medrud, S. I. Zones, *J. Am. Chem. Soc.* **2000**, *122*, 263–273.
- [102] Y. Nakagawa, S. I. Zones in *Synthesis of Microporous Materials, Band 1* (Ed.: M. L. Occelli, H. Robson), Van Nostrand Reinhold, New York, **1992**, p. 222.
- [103] S. I. Zones, R. J. Darton, R. Morris, S. J. Hwang, *J. Phys. Chem. B* **2005**, *109*, 652–661.
- [104] S. I. Zones, A. W. Burton, G. S. Lee, M. M. Olmstead, *J. Am. Chem. Soc.* **2007**, *129*, 9066–9079.

- [105] S. I. Zones, Y. Nakagawa, L. T. Yuen, T. V. Harris, *J. Am. Chem. Soc.* **1996**, *118*, 7558–7567.
- [106] C. David, C. Jane, US Pat 6049018, **2000**.
- [107] G. S. Lee, S. I. Zones, *J. Solid State Chem.* **2002**, *167*, 289.
- [108] a) G. W. Dodwell, R. P. Denkwicz, L. B. Sand, *Zeolites* **1985**, *5*, 153; b) N. A. Briscoe, D. W. Johnson, M. D. Shannon, G. T. Kokotailo, L. B. McCusker, *Zeolites* **1988**, *8*, 74–76.
- [109] A. Moini, K. D. Schmitt, E. W. Valyocsik, R. F. Polomski, *Zeolites* **1994**, *14*, 504–511.
- [110] a) A. Corma, M. Puche, F. Rey, G. Sankar, S. J. Teat, *Angew. Chem.* **2003**, *115*, 1188–1191; *Angew. Chem. Int. Ed.* **2003**, *42*, 1156–1159; b) J. A. Vidal-Moya, T. Blasco, F. Rey, A. Corma, M. Puche, *Chem. Mater.* **2003**, *15*, 3961–3963.
- [111] A. Corma, M. T. Navarro, F. Rey, J. Rius, S. Valencia, *Angew. Chem.* **2001**, *113*, 2337; *Angew. Chem. Int. Ed.* **2001**, *40*, 2277.
- [112] Y. Mathieu, J. L. Paillaud, P. Caullet, N. Bats, *Microporous Mesoporous Mater.* **2004**, *75*, 13–22.
- [113] A. Corma, F. Rey, S. Valencia, J. L. Jordá, J. Rius, *Nat. Mater.* **2003**, *2*, 493.
- [114] R. Castañeda, A. Corma, V. Fornés, F. Rey, J. Rius, *J. Am. Chem. Soc.* **2003**, *125*, 7820.
- [115] M. Afeworki, D. L. Dorset, G. J. Kennedy, K. G. Strohmaier, *Chem. Mater.* **2006**, *18*, 1697–1704.
- [116] M. Matsukata, N. Nishiyama, K. Ueyama, *Microporous Mater.* **1993**, *1*, 219.
- [117] M. H. Kim, H. X. Li, M. E. Davis, *Microporous Mater.* **1993**, *1*, 191–200.
- [118] M. Matsukata, M. Ogura, T. Osaki, P. R. H. P. Rao, M. Nomura, E. Kikuchi, *Top. Catal.* **1999**, *9*, 77–92.
- [119] W. Y. Xu, J. X. Dong, J. P. Li, J. Q. Li, F. Wu, *J. Chem. Soc. Chem. Commun.* **1990**, 755.
- [120] P. R. H. P. Rao, K. Ueyama, M. Matsukata, *Appl. Catal. A* **1998**, *166*, 97–103.
- [121] Y. Koyama, T. Ikeda, T. Tatsumi, Y. Kubota, *Angew. Chem.* **2008**, *120*, 1058–1062; *Angew. Chem. Int. Ed.* **2008**, *47*, 1042–1046.
- [122] M. A. Cambor, A. Corma, S. Valencia, *Chem. Commun.* **1996**, 2365–2366.
- [123] M. J. Díaz-Cabañas, P. A. Barrett, M. A. Cambor, *Chem. Commun.* **1998**, 1881.
- [124] E. M. Flanigen, R. L. Patton, US Pat 4073865, **1978**.
- [125] a) J. L. Guth, H. Kessler, R. Wey, *Stud. Surf. Sci. Catal.* **1986**, *28*, 121; b) J. L. Guth, P. Caullet, A. Seive, J. Patarin, F. Delprato, *Guidelines in Mastering the Properties of Molecular Sieves*. Plenum, New York, **1990**, p. 69; c) A. Merrouche, J. Patarin, M. Soulard, H. Kessler, D. Anglerot, in *Synthesis of Microporous Molecular Sieves* (Ed.: M. L. Occelli, H. Robson), Van Nostrand Reinhold, New York, **1992**, p. 384; d) J. L. Guth, H. Kessler, P. Caullet, J. Hazm, A. Merrouche, J. Patarin, *Proc. 9th Int. Zeolite Conf.*, Montreal, Butterworth-Heinemann, **1993**, p. 215; e) J. L. Guth, H. Kessler, J. M. Higel, J. M. Lamblin, J. Patarin, A. Seive, J. M. Chezeau, R. Wey, *ACS Symp. Ser.* **1998**, *398*, 176.
- [126] a) J. Song, H. Gies, *Stud. Surf. Sci. Catal.* **2004**, *154A*, 295; b) M. A. Cambor, L. A. Villaescusa, M. J. Díaz-Cabañas, *Top. Catal.* **1999**, *9*, 59.
- [127] M. A. Cambor, P. A. Barrett, M. J. Díaz-Cabañas, L. A. Villaescusa, M. Puche, T. Boix, E. Perez, H. Koller, *Microporous Mesoporous Mater.* **2001**, *48*, 11–22.
- [128] I. Krutskaya, *Russ. J. Inorg. Chem.* **1998**, *30*, 438.
- [129] R. Millini, G. Perego, G. Bellussi, *Top. Catal.* **1999**, *9*, 13–34.
- [130] D. L. Dorset, G. J. Kennedy, *J. Phys. Chem. B* **2005**, *109*, 13891–13898.
- [131] P. Wagner, O. Terasaki, S. Ritsch, J. G. Nery, S. I. Zones, M. E. Davis, K. Hiraga, *J. Phys. Chem. B* **1999**, *103*, 8245–8250.
- [132] S. Elomari, A. Burton, R. C. Medrud, R. G. Kunstleve, *Microporous Mesoporous Mater.* **2009**, *118*, 325–333.
- [133] Y. F. Li, X. D. Zou, *Angew. Chem.* **2005**, *117*, 2048–2051; *Angew. Chem. Int. Ed.* **2005**, *44*, 2012–2015.
- [134] A. Burton, S. Elomari, *Chem. Commun.* **2004**, 2618–2619.
- [135] S. Elomari, A. W. Burton, K. Ong, A. R. Pradhan, I. Y. Chan, *Chem. Mater.* **2007**, *19*, 5485–5492.
- [136] J. Annen, M. E. Davis, J. B. Higgins, J. L. Schlenker, *J. Chem. Soc. Chem. Commun.* **1991**, 1175.
- [137] L. B. McCusker, R. W. G. Kunstleve, C. Baerlocher, M. Yoshikawa, M. E. Davis, *Microporous Mater.* **1996**, *6*, 295–309.
- [138] C. Röhrig, H. Gies, *Angew. Chem.* **1995**, *107*, 125; *Angew. Chem. Int. Ed. Engl.* **1995**, *34*, 63.
- [139] H. L. Li, O. M. Yaghi, *J. Am. Chem. Soc.* **1998**, *120*, 10569.
- [140] T. Conradsson, M. S. Dadachov, X. D. Zou, *Microporous Mesoporous Mater.* **2000**, *41*, 183.
- [141] a) T. Blasco, A. Corma, M. J. Díaz-Cabañas, F. Rey, J. A. Vidal-Moya, C. M. Zicovich-Wilson, *J. Phys. Chem. B* **2002**, *106*, 2634–2642; b) A. Corma, M. J. Díaz-Cabañas, V. Fornés, *Angew. Chem.* **2000**, *112*, 2436; *Angew. Chem. Int. Ed.* **2000**, *39*, 2346; c) L. A. Villaescusa, P. A. Barret, M. A. Cambor, *Angew. Chem.* **1999**, *111*, 2164; *Angew. Chem. Int. Ed.* **1999**, *38*, 1997; d) A. Cantín, A. Corma, M. J. Díaz-Cabañas, F. Rey, G. Sastre, *Stud. Surf. Sci. Catal.* **2004**, *154*, 481–488.
- [142] a) A. Cantin, A. Corma, M. J. Díaz-Cabañas, J. L. Jordá, M. Moliner, F. Rey, *Angew. Chem.* **2006**, *118*, 8181–8183; *Angew. Chem. Int. Ed.* **2006**, *45*, 8013–8015; b) Z. Liu, T. Ohsuna, O. Terasaki, M. A. Cambor, M. J. Díaz-Cabañas, K. Hiraga, *J. Am. Chem. Soc.* **2001**, *123*, 5370–5371.
- [143] a) A. Corma, M. J. Díaz-Cabañas, L. J. Martínez-Triguero, F. Rey, J. Rius, *Nature* **2002**, *418*, 514; b) T. Blasco, A. Corma, M. J. Díaz-Cabañas, F. Rey, J. Rius, G. Sastre, J. A. Vidal-Moya, *J. Am. Chem. Soc.* **2004**, *126*, 13414–13423.
- [144] D. E. W. Vaughan, K. G. Strohmaier, US Pat 5455020, **1995**.
- [145] M. Moliner, M. J. Díaz-Cabañas, V. Fornés, C. Martínez, A. Corma, *J. Catal.* **2008**, *254*, 101–109.
- [146] A. Corma, M. J. Díaz-Cabañas, J. L. Jordá, F. Rey, G. Sastre, K. G. Strohmaier, *J. Am. Chem. Soc.* **2008**, *130*, 16482–16483.
- [147] A. Taguchi, F. Schüth, *Microporous Mesoporous Mater.* **2005**, *77*, 1–45.
- [148] T. Yamada, H. S. Zhou, I. Honma, Y. Ueno, T. Horiuchi, O. Niwa, *Chem. Lett.* **2005**, *34*, 328–329.
- [149] M. Vallet-Regí, F. Balas, D. Arcos, *Angew. Chem.* **2007**, *119*, 7692–7703; *Angew. Chem. Int. Ed.* **2007**, *46*, 7548–7558.
- [150] M. V. Regi, M. Colilla, I. I. Barba, *J. Biomed. Nanotechnol.* **2008**, *4*, 1–15.
- [151] S. N. Kim, W. J. Son, J. S. Choi, W. S. Ahn, *Microporous Mesoporous Mater.* **2008**, *115*, 497–503.
- [152] J. L. Shen, C. F. Cheng, *Curr. Opin. Solid State Mater. Sci.* **2003**, *7*, 427–433.
- [153] C. Y. Chen, H. X. Li, M. E. Davis, *Microporous Mater.* **1993**, *2*, 17–26.
- [154] A. Corma, V. Fornés, M. T. Navarro, J. Perezpariente, *J. Catal.* **1994**, *148*, 569–574.
- [155] K. R. Kloetstra, H. Bekkum, J. C. Jansen, *Chem. Commun.* **1997**, 2281–2282.
- [156] Y. Liu, T. J. Pinnavaia, *Chem. Mater.* **2002**, *14*, 3–5.
- [157] Z. T. Zhang, Y. Han, F. S. Xiao, S. L. Qiu, L. Zhu, R. W. Wang, Y. Yu, Z. Zhang, B. S. Zou, Y. Q. Wang, H. P. Sun, D. Y. Zhao, Y. Wei, *J. Am. Chem. Soc.* **2001**, *123*, 5014–5021.
- [158] J. L. Sun, C. Bonneau, A. Cantin, A. Corma, M. J. Díaz-Cabañas, M. Moliner, D. L. Zhang, M. R. Li, X. D. Zou, *Nature* **2009**, *458*, 1154–1159.
- [159] M. J. Climent, A. Corma, A. Velty, *Appl. Catal. A* **2004**, *263*, 155–161.
- [160] V. Valtchev, personal communication.
- [161] H. X. Li, M. E. Davis, *Catal. Today* **1994**, *19*, 61–106.
- [162] M. Hartmann, L. Kevan, *Chem. Rev.* **1999**, *99*, 635–664.

- [163] B. K. Czarnetzki, R. J. Dogterom, W. H. J. Stork, K. A. Emeis, J. P. V. B. Houckgeest, *J. Catal.* **1993**, *141*, 140–147.
- [164] J. A. Martens, H. Geerts, L. Leplat, G. Vanbutsele, P. J. Grobet, P. A. Jacobs, *Catal. Lett.* **1992**, *12*, 367–374.
- [165] Y. I. Isakov, K. M. Minachev, R. Tome, A. Tissler, G. Oehlmann, V. P. Kalinin, T. A. Isakova, *Russ. Chem. Bull.* **1994**, *43*, 2004–2010.
- [166] K. Roos, A. Liepold, H. Koch, W. Reschetilowski, *Chem. Eng. Technol.* **1997**, *20*, 326–332.
- [167] B. Y. Hsu, S. Cheng, J. M. Chen, *J. Mol. Catal. A* **1999**, *149*, 7–23.
- [168] J. Schripsema, C. R. R. Matos, C. R. Oliveira, C. B. Rodella, F. J. Luna, *Catal. Commun.* **2003**, *4*, 229–235.
- [169] T. L. Barr, J. Klinowski, H. Y. He, K. Alberti, G. Müller, J. A. Lercher, *Nature* **1993**, *365*, 429–431.
- [170] A. Janin, J. C. Lavalley, E. Benazzi, C. Schott-Daries, H. Kessler, *Catal. Microporous Mater. Stud. Surf. Sci. Catal.* **1995**, *94*, 124–130.
- [171] G. Mueller, G. Edermirth, H. Kessler, J. A. Lercher, *J. Phys. Chem.* **1995**, *99*, 12327–12331.
- [172] M. Richter, H. Fischer, M. Bartoszek, H. L. Zubowa, R. Fricke, *Microporous Mater.* **1997**, *8*, 69–78.
- [173] J. Datka, B. Gil, *Catal. Today* **2001**, *70*, 131–138.
- [174] C. Y. Chen, S. I. Zones, *Stud. Surf. Sci. Catal.* **2001**, *135*, 2855–2861.
- [175] C. Y. Chen, S. I. Zones, A. W. Burton, S. A. Elomari, S. Svelle, *Stud. Surf. Sci. Catal.* **2007**, *172*, 329.
- [176] a) A. Corma, E. Sastre, *J. Chem. Soc. Chem. Commun.* **1991**, 594–596; b) A. Corma, E. Sastre, *J. Catal.* **1991**, *129*, 177–185; c) A. Corma, F. Llopis, J. B. Monton, *Stud. Surf. Sci. Catal.* **1993**, *75*, 1145.
- [177] C. W. Jones, S. I. Zones, M. E. Davis, *Appl. Catal. A* **1999**, *181*, 289–303.
- [178] a) J. Weitkamp, S. Ernst, *Catal. Today* **1994**, *19*, 107–150; b) B. Adair, C. Y. Chen, K. T. Wan, M. E. Davis, *Microporous Mater.* **1996**, *7*, 261–270.
- [179] J. A. Martens, J. P. Pariente, E. Sastre, A. Corma, P. A. Jacobs, *Appl. Catal. A* **1988**, *45*, 85–101.
- [180] D. E. De Vos, S. Ernst, C. Perego, C. T. O'Connor, M. Stöcker, *Microporous Mesoporous Mater.* **2002**, *56*, 185–192.
- [181] S. Tontisirin, S. Ernst, *Angew. Chem.* **2007**, *119*, 7443–7446; *Angew. Chem. Int. Ed.* **2007**, *46*, 7304–7306.
- [182] a) H. G. Karge, J. Ladebeck, Z. Sarbak, K. Hatada, *Zeolites* **1982**, *2*, 94–102; b) H. G. Karge, K. Hatada, Y. Zhang, R. Fiedorow, *Zeolites* **1983**, *3*, 13–21.
- [183] J. Weitkamp, S. Ernst, P. A. Jacobs, H. G. Karge, *Erdoel Kohle Erdgas Petrochem.* **1986**, *39*, 13–18.
- [184] J. Weitkamp, S. Ernst in *Guidelines for Mastering the Properties of Molecular Sieves* (Eds.: D. Barthomeuf, E. G. Derouane, W. Hölderich), Plenum, New York, **1990**, S. 343–353.
- [185] J. Weitkamp, S. Ernst, R. Kumar, *Appl. Catal.* **1986**, *27*, 207–210.
- [186] J. Martinez-Triguero, M. J. Diaz-Cabañas, M. A. Cambor, V. Fornés, T. L. M. Maesen, A. Corma, *J. Catal.* **1999**, *182*, 463–469.
- [187] a) Y. Sugi, Y. Kubota, T. A. Hanaoka, T. Matsuzaki, *Catal. Surv. Jpn.* **2001**, *5*, 43–56; b) Y. Kubota, S. Tawada, K. Nakagawa, C. Naitoh, N. Sugimoto, Y. Fukushima, T. Hanaoka, Y. Imada, Y. Sugi, *Microporous Mesoporous Mater.* **2000**, *37*, 291–301; c) Y. Sugi, Y. Kubota, A. Ito, H. Maekawa, R. K. Ahedi, S. Tawada, S. Watanabe, I. Toyama, C. Asaoka, H. S. Lee, J. H. Kim, G. Seo, *Stud. Surf. Sci. Catal.* **2004**, *154*, 2228–2238; d) H. Maekawa, C. Naitoh, K. Nakagawa, A. Iida, K. Komura, K. Yoshihiro, Y. Sugi, J. H. Kim, G. Seob, *J. Mol. Catal. A* **2007**, *274*, 24–32; e) Y. Sugi, H. Maekawa, S. A. R. Mulla, A. Ito, C. Naitoh, K. Nakagawa, K. Komura, Y. Kubota, J. H. Kim, G. Seo, *Bull. Chem. Soc. Jpn.* **2007**, *80*, 1418–1428.
- [188] a) K. J. Balkus, A. Khanmamedova, A. G. Gabrielov, S. I. Zones, *Stud. Surf. Sci. Catal.* **1996**, *101*, 1341; b) K. J. Balkus, A. K. Khanmamedova in *3rd World Congress on Oxidation Catalysis, Vol. 110* (Eds.: R. K. Grasselli, S. T. Oyama, A. M. Gaffney, J. E. Lyons), Elsevier, Dordrecht, **1997**, p. 1007–1014.
- [189] a) M. J. Climent, A. Corma, A. Velty, *J. Catal.* **2000**, *196*, 345–351; b) M. J. Climent, A. Corma, A. Velty, *Green Chem.* **2002**, *4*, 565–569; c) M. J. Climent, A. Corma, A. Velty, *Appl. Catal. A* **2004**, *263*, 155–161.
- [190] I. D. Williams, J. H. Yu, H. B. Du, J. S. Chen, W. Q. Pang, *Chem. Mater.* **1998**, *10*, 773–776.
- [191] W. T. Yang, J. Y. Li, Q. H. Pan, Z. Jin, J. H. Yu, R. R. Xu, *Chem. Mater.* **2008**, *20*, 4900–4905.
- [192] S. Natarajan, S. Neeraj, A. Choudhury, C. N. R. Rao, *Inorg. Chem.* **2000**, *39*, 1426–1433.
- [193] M. Cavellec, J. M. Greneche, D. Riou, G. Ferey, *Microporous Mater.* **1997**, *8*, 103–112.
- [194] A. Thirumurugan, S. Natarajan, *Dalton Trans.* **2003**, 3387–3391.
- [195] J. A. Rodgers, W. T. A. Harrison, *J. Mater. Chem.* **2000**, *10*, 2853–2856.
- [196] K. H. Lii, Y. F. Huang, *Chem. Commun.* **1997**, 839–840.
- [197] G. Y. Yang, S. C. Sevov, *J. Am. Chem. Soc.* **1999**, *121*, 8389–8390.
- [198] A. Choudhury, S. Natarajan, C. N. R. Rao, *Chem. Commun.* **1999**, 1305–1306.
- [199] M. A. Cambor, A. Corma, P. Lightfoot, L. A. Villaescusa, P. A. Wright, *Angew. Chem.* **1997**, *109*, 2774–2776; *Angew. Chem. Int. Ed. Engl.* **1997**, *36*, 2659–2661.
- [200] a) P. A. Barrett, M. A. Cambor, A. Corma, R. H. Jones, L. A. Villaescusa, *Chem. Mater.* **1997**, *9*, 1713–1715; b) P. A. Barrett, M. A. Cambor, A. Corma, R. H. Jones, L. A. Villaescusa, *J. Phys. Chem. B* **1998**, *102*, 4147–4155.
- [201] L. A. Villaescusa, P. A. Barrett, M. A. Cambor, *Chem. Commun.* **1998**, 2329–2330.
- [202] P. A. Barrett, T. Boix, M. Puche, D. H. Olson, E. Jordan, H. Koller, M. A. Cambor, *Chem. Commun.* **2003**, 2114–2115.
- [203] A. Cantin, A. Corma, S. Leiva, F. Rey, J. Rius, S. Valencia, *J. Am. Chem. Soc.* **2005**, *127*, 11560–11561.